

## 6 FIRST ORDER OPTICS

## 6.1 GENERAL

**6.1.1 First order optics and paraxial rays.** In Section 5.11.2 it was pointed out that when the sine of the angle is replaced by the angle, the resulting equations belong to the field of first order optics. In general, if any trigonometric function is replaced by its first approximation, we get first order equations, in the field of optics. In Sections 5.9.1 and 5.9.2 we defined a paraxial ray as one differentially displaced from the optical axis. Because of this definition we must use the first approximation to the trigonometric functions in the equations for a differentially traced ray. The resulting paraxial ray equations are hence identical to the first order equations.

**6.1.2 Preliminary layout and graphical ray trace.** The method of tracing paraxial rays graphically was explained in Section 5.10. Graphical ray tracing is extremely useful in the preliminary design stage, particularly for complicated systems, which cannot be visualized easily. The designer can thereby get a "feel" for the system, which a mere array of numbers often hides. Graphical ray tracing, however, is limited to an accuracy of about one percent. For additional accuracy, which is absolutely necessary in the calculation of aberrations, we must resort to numerical paraxial ray tracing. The methods and results of this type of ray tracing in the realm of first order optics will be discussed in Section 6.

## 6.2 NUMERICAL TRACING OF PARAXIAL RAYS

**6.2.1 Importance of paraxial ray tracing.** The accurate numerical tracing of paraxial rays is used extensively in the design of optical systems for three main reasons:

- (1) Tracing paraxial rays through the system is a simple mathematical procedure.
- (2) Images formed by paraxial rays provide very convenient reference planes.
- (3) Data obtained in paraxial ray calculations can be used to calculate the first approximation to image aberration.

For these reasons, a systematic method of numerical ray tracing of paraxial rays is a necessary tool for the designer, even today when large automatic computers are readily available. In this section such a method will be described; and it will be used extensively in the following sections to illustrate the vast amount of information made available by paraxial ray tracing.

## 6.2.2 Ray trace format.


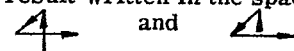
**6.2.2.1** The first step in tracing a paraxial ray is to lay out the system data in a form as shown in the top of Table 5.1. Then the two constants,  $c(n_{-1} - n)$  and  $t/n$ , are computed for each surface and space respectively. (See Table 6.1). With these constants filled in, the paraxial ray may be traced by applying Equations (56) and (57) of Section 5.

**6.2.2.2** As one uses this representation, its value becomes evident. These equations, and the way the data

| SURFACE       | 0         | 1              | 2              | 3 etc. |
|---------------|-----------|----------------|----------------|--------|
| c             | $c_0$     | $c_1$          | $c_2$          | $c_3$  |
| t             | $t_0$     | $t_1$          | $t_2$          |        |
| n             | $n_0$     | $n_1$          | $n_2$          |        |
| $c(n_{-1}-n)$ |           | $c_1(n_0-n_1)$ | $c_2(n_1-n_2)$ |        |
| $t/n$         | $t_0/n_0$ | $t_1/n_1$      | $t_2/n_2$      |        |
| y             | $y_0$     | $y_1$          | $y_2$          |        |
| nu            | $n_0 u_0$ | $n_1 u_1$      | $n_2 u_2$      |        |

Table 6.1 - Recommended format for tracing paraxial rays through an optical system.

are laid out, make almost a perfect match with the requirements of a desk calculator. A few of these features are:

- (1) In calculating  $c(n_{-1} - n)$  one obtains the data from a triangle of numbers, 
- (2) In tracing the ray, both equations are computed in the same way. First a number is multiplied by a number directly above it, then the product added to the number below the double line on the left, and the result written in the space on the right. This is indicated by the lines shown in the figure that appear as 

(3) Many times, problems are worked backwards. For example, suppose  $n_{-1} u_{-1}$ ,  $nu$ , and  $y$  are given, and the problem is to find  $c$ . The question is: how to remember what to do first, i.e., divide  $y$  by  $(nu - n_{-1} u_{-1})$ , or vice versa? It turns out that the correct method is always the easiest one to do on the calculating machine. Dividing  $(nu - n_{-1} u_{-1})$  by  $y$  can be done without writing down  $(nu - n_{-1} u_{-1})$ . However, to calculate  $y/(nu - n_{-1} u_{-1})$ , the difference must be written down; therefore, we know that to calculate  $c$ , the result must be  $(nu - n_{-1} u_{-1})/y$  divided by  $(n_{-1} - n)$ . As another example, suppose a value of  $y_1$ ,  $y_2$ , and  $n_1 u_1$  are given, what  $t_1/n_1$  is needed? The formula can be remembered in the following way: first compute  $y_2 - y_1$ , and then divide by  $n_1 u_1$ . Therefore the formula is  $t_1/n_1 = (y_2 - y_1)/n_1 u_1$ .

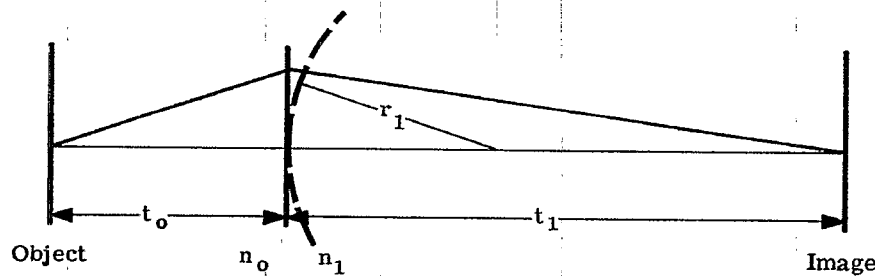


Figure 6.1 - Relation between image and object points.

6.2.3 Algebraic example. Table 6.1 may also be used to derive algebraic expressions useful in optics. One can very readily work out the equation for image and object distances for a single refracting surface. If a surface of radius  $r_1$  separates two media of index  $n_o$  and  $n_1$ , an object point will be imaged at a distance  $t_1$  from the surface (see Figure 6.1). What is the relation between  $t_o$  and  $t_1$ ? This is a three surface problem, the object surface, 0, the refracting surface, 1, and the image surface, 2. A paraxial ray at  $y_o = 0$  will be imaged at  $y_2 = 0$ . It is therefore possible to fill out the calculations of Table 6.1 to the following extent. (See Table 6.2).

| SURFACE         | OBJECT | 1                | IMAGE     |
|-----------------|--------|------------------|-----------|
| $c$             | 0      | $c_1$            | 0         |
| $t$             |        | $t_o$            | $t_1$     |
| $n$             |        | $n_o$            | $n_1$     |
| $c(n_{-1} - n)$ | 0      | $c_1(n_o - n_1)$ | 0         |
| $t/n$           |        | $t_o/n_o$        | $t_1/n_1$ |
| $y$             | 0      |                  | 0         |
| $nu$            |        |                  |           |

Table 6.2 - Single refracting surface, axial object and image points.

Now, as pointed out in Sections 5.9.3 and 5.10.1, the angle used to trace a paraxial ray does not affect the image position. Since the choice of  $y$  on the lens is arbitrary, let it be  $y_1$ . The calculations to this point are shown in Table 6.3.

|                          |   |                  |           |
|--------------------------|---|------------------|-----------|
| $c(n_{-1} - n)$<br>$t/n$ | 0 | $c_1(n_o - n_1)$ | 0         |
| $y$<br>$nu$              | 0 | $y_1$            | 0         |
|                          |   | $t_o/n_o$        | $t_1/n_1$ |
|                          |   | $n_o u_o$        | $n_1 u_1$ |

Table 6.3 - Continuation of Table 6.2.

With  $y_o (=0)$  and  $y_1$  (arbitrary) known,  $n_o u_o = (y_1 - 0)/(t_o/n_o)$ .

With  $n_o u_o$  and  $y_1$  known,  $n_1 u_1 = n_o u_o + y_1 c_1 (n_o - n_1)$ .

With  $n_1 u_1$ ,  $y_1$  and  $y_2 (=0)$  known,  $t_1/n_1 = (0 - y_1)/n_1 u_1$ .

Therefore  $t_1/n_1 = -y_1/n_1 u_1$ , or

$$\frac{n_1}{t_1} = -\frac{n_1 u_1}{y_1} = \frac{-n_o u_o}{y_1} - c_1 (n_o - n_1) = -\frac{n_o}{t_o} + c_1 (n_1 - n_o).$$

This equation becomes the familiar refraction equation, derived in Paragraph 5.9.3.2,

$$\frac{n_1}{t_1} + \frac{n_o}{t_o} = c_1 (n_1 - n_o). \tag{1}$$

Notice how the  $y_1$  has dropped out of the equation indicating that any value  $y_1$  could have been used. The calculations will be finally filled out in Table 6.4 as follows:

|             |   |                         |               |
|-------------|---|-------------------------|---------------|
| $y$<br>$nu$ | 0 | $y_1$                   | 0             |
|             |   | $y_1 n_o/t_o$           | $y_1 n_o/t_o$ |
|             |   | $+ y_1 c_1 (n_o - n_1)$ |               |

Table 6.4 - Conclusion of Table 6.3.

6.2.4 Numerical example. Equation (1) was given to show how the ray trace table can be used to derive a classical formula. Actually one will find very little occasion to use Equation (1) to calculate a numerical result, because problems can be solved much more readily using the format of Table 6.1. For example, suppose one is given the problem  $c_1 = 0.10$ ,  $n_o = 1$ ,  $n_1 = 1.5$ ,  $t_o = 10$ . Rather than remember any special formula, go directly to the format as shown in Table 6.5.

| SURFACE                  | OBJECT | 1         | IMAGE |
|--------------------------|--------|-----------|-------|
| $c$                      | 0      | 0.10      | 0     |
| $t$                      | 10     | $t_1$     |       |
| $n$                      | 1      | 1.5       |       |
| $c(n_{-1} - n)$<br>$t/n$ | 0      | -0.05     | 0     |
|                          | 10     | $t_1/1.5$ |       |
| $y$<br>$nu$              | 0      | 1         | 0     |
|                          | 0.10   | 0.05      |       |

$$(0.05) \frac{t_1}{1.5} + 1 = 0$$

$$\frac{t_1}{1.5} = \frac{-1}{.05} = -20$$

$$t_1 = (1.5) (-20) = -30$$

Table 6.5 - Numerical example of a single refracting surface.

6.2.5 Ray trace for three element lens. Table 6.6 shows the data and ray trace results for a three element lens. All the material above the lowest double line has been discussed earlier in this chapter. The last two lines, involving  $\bar{y}$  and  $n\bar{u}$ , and the calculations of  $m$  (lateral magnification),  $f'$  (focal length), and  $\Phi$  (optical invariant) will be discussed in the following sections.

| SURFACE         | OBJECT<br>0 | 1        | 2        | 3        | 4        | 5        | 6        | IMAGE<br>7 |
|-----------------|-------------|----------|----------|----------|----------|----------|----------|------------|
| c               | 0           | 0.25285  | -0.01474 | -0.19942 | 0.25973  | 0.05065  | -0.24588 | 0          |
| t               |             | 25.00000 | 0.60000  | 1.06541  | 0.15000  | 1.13691  | 0.60000  | 14.05015   |
| n               |             | 1.00000  | 1.62000  | 1.00000  | 1.62100  | 1.00000  | 1.62000  | 1.00000    |
| $c(n_{-1} - n)$ |             | -0.15677 | -0.00914 | 0.12384  | 0.16129  | -0.03140 | -0.15245 |            |
| $t/n$           |             | 25.00000 | 0.37037  | 1.06541  | 0.09254  | 1.13691  | 0.37037  | 14.05015   |
| y               | 0           | 1.25000  | 1.19594  | 1.02879  | 1.02606  | 1.18070  | 1.21734  | 0          |
| nu              |             | 0.05000  | -0.14596 | -0.15689 | -0.02948 | 0.13601  | 0.09894  | -0.08664   |
| $\bar{y}$       | -10.00000   | -0.75000 | -0.56942 | -0.04440 | 0.00069  | 0.55481  | 0.72887  | 5.77084    |
| $n\bar{u}$      |             | 0.37000  | 0.48758  | 0.49278  | 0.48728  | 0.48739  | 0.46997  | 0.35886    |

$$m = \frac{n_o u_o}{n_6 u_6} = -0.57708 = \frac{\bar{y}_7}{y_o} \quad \Phi = -0.50000$$

$$f' = -\frac{\Phi}{n_o (u_o \bar{u}_6 - \bar{u}_o u_6)} = \frac{0.5}{1 (0.05 \times 0.35886 + 0.37 \times 0.08664)} = 10.000$$

Table 6.6 Sample calculation of paraxial rays through a three element lens, using Equations 5-(56) and 5-(57).

6.2.6 Ray trace procedure for calculation of aberrations. Another way to trace paraxial rays is to use the following equations:

$$y = y_{-1} + t_{-1} u_{-1} \tag{2}$$

$$u = u_{-1} + i \left[ \frac{(n_{-1}/n) - 1}{n} \right] \tag{3}$$

This ray trace involves the new quantity,  $i$ , which is the limiting value of the angle of incidence,  $I$ , as the ray approaches the axis in the paraxial region. Equation (2) is merely Equation 5-(56) simplified. Equation (3) comes from Equation 5-(35), written for small angles, with the substitution  $i' = i n_{-1}/n$ ; the latter is the law of refraction for small angles. Now from Figure 5.11,  $I' - U =$  the acute angle between  $r$  and the optical axis. But for small angles this is  $y/r = y/c$ . Hence, using Equation 5-(35) we have,

$$i = y/c + u_{-1} \tag{4}$$

It will be shown later (Section 8) how the third order aberrations may be calculated from paraxial ray data. For these calculations it is easier to use Equations (2), (3) and (4), than Equations 5-(56) and 5-(57).

6.2.7 Numerical example.

6.2.7.1 To illustrate these equations, Table 6.7 includes paraxial rays traced through the same lens as used in Table 6.6. In this example, a different set of rays are traced through the lens. Below the lowest double line there are entries used in the calculation of chromatic aberration. These calculations will be explained in Section 6.10.

| SURFACE                               | OBJECT<br>0 | 1         | 2         | 3         | 4         | 5         | 6         | IMAGE<br>7            |
|---------------------------------------|-------------|-----------|-----------|-----------|-----------|-----------|-----------|-----------------------|
| c                                     | 0           | 0.252850  | -0.014740 | -0.199420 | 0.259730  | 0.050650  | -0.245880 |                       |
| t                                     | $\infty$    | 0.600000  | 1.065410  | 0.150000  | 1.136910  | 0.600000  | 8.279369  |                       |
| n                                     | 1.000000    | 1.620000  | 1.000000  | 1.621000  | 1.000000  | 1.620000  | 1.000000  |                       |
| $(n_{-1} / n) - 1$                    |             | -0.382716 | 0.620000  | -0.383097 | 0.621000  | -0.382716 | 0.620000  |                       |
| y                                     | 0           | 1.500000  | 1.412907  | 1.148619  | 1.138827  | 1.227353  | 1.241918  | 0                     |
| u                                     | 0           | -0.145155 | -0.248063 | -0.065279 | 0.077866  | 0.024274  | -0.150001 |                       |
| i                                     |             | 0.379275  | -0.165981 | -0.477120 | 0.230508  | 0.140031  | -0.281089 |                       |
| $dn/n$                                | 0           | 0.006370  | 0         | 0.010586  | 0         | 0.006370  |           | $T_{Ach} = -0.0029$   |
| $\Delta(dn/n)$                        |             | 0.006370  | -0.006370 | 0.010586  | -0.010586 | 0.006370  | -0.006370 | $\Sigma a = -0.00044$ |
| $a = -y n_{-1} i \Delta \frac{dn}{n}$ |             | -0.00362  | -0.00242  | 0.00580   | 0.00450   | -0.00109  | -0.00360  |                       |

Table 6.7 - A paraxial ray is traced through the same lens as used in Table 6.6. In this case Equations (2), (3), and (4) are used.

6.2.7.2 For use with a large computing machine there is no preference for either of these methods. For hand computing, unless aberrations are calculated, the method outlined in Table 6.1 is simpler. Therefore, all the paraxial ray theory given in Section 6.3-6.9 will be based on Equations 5-(56) and 5-(57).

### 6.3 THE OPTICAL INVARIANT

6.3.1 Axial and oblique rays. In Section 6.2 it was shown how images may be located along the axis of the optical system. The procedure is to trace a paraxial ray from where the object surface crosses the optical axis ( $y_o = 0$ ). Such a ray is called an axial paraxial ray. An image surface is formed wherever this paraxial ray crosses the optical axis. By tracing a second ray from the object at a value of  $y_o \neq 0$  it is possible also to determine the size of the image. Such a ray is called an oblique paraxial ray. The data for this second ray will be identified by writing  $y$  and  $\bar{u}$ . Table 6.6 shows a second ray traced through the lens. The second ray is commonly referred to as the oblique paraxial ray because it passes from an off-axis object point obliquely through the optical system to the image. If this ray passes through the center of the aperture stop it is called a chief ray. In tracing the oblique paraxial and the axial paraxial ray through the system, the following equations have been applied for each surface:

$$nu = n_{-1} u_{-1} + yc (n_{-1} - n) \quad \text{for the axial paraxial ray refraction.} \quad 5-(57a)$$

$$n\bar{u} = n_{-1} \bar{u}_{-1} + \bar{y}c (n_{-1} - n) \quad \text{for the oblique paraxial ray refraction.} \quad 5-(57b)$$

$$y = y_{-1} + \frac{t_{-1}}{n_{-1}} (n_{-1} u_{-1}) \quad \text{for the axial paraxial ray transfer.} \quad 5-(56a)$$

$$\bar{y} = \bar{y}_{-1} + \frac{t_{-1}}{n_{-1}} (n_{-1} \bar{u}_{-1}) \quad \text{for the oblique paraxial ray transfer.} \quad 5-(56b)$$

6.3.2 The optical invariant and its importance. We will use the last four equations, involving axial and oblique paraxial rays, to derive an expression called the optical invariant. This quantity, as its name implies, is a constant; as such it may be calculated in several ways and its value for a given system can be used in the calculation of various quantities. This invariant has a meaning for an optical system similar to momentum or energy for an isolated mechanical system.

6.3.3 The invariant for refraction. By transposition and division, using Equations 5-(57a) and 5-(57b), it is possible to equate the common term  $c (n_{-1} - n)$  giving

$$\frac{nu - n_{-1} u_{-1}}{y} = \frac{n\bar{u} - n_{-1} \bar{u}_{-1}}{\bar{y}}$$

By rearranging, this may be written

$$\bar{y} (n_{-1} u_{-1}) - y (n_{-1} \bar{u}_{-1}) = \bar{y} (nu) - y (n\bar{u}) \quad (5)$$

The index and angle data on the left side of this equation refer to the space to the left of the surface, and the corresponding data on the right side refer to the space to the right of the surface. This equation shows that

$$\bar{y} (nu) - y (n\bar{u}) = \Phi \quad (6)$$

is an invariant for the refraction at any surface in the optical system.  $\Phi$  is called the optical invariant.

6.3.4 The invariant for transfer. In a similar way Equations 5-(56a) and 5-(56b) may be combined to give the relation

$$\bar{y}_{-1} (n_{-1} u_{-1}) - y_{-1} (n_{-1} \bar{u}_{-1}) = \bar{y} (n_{-1} u_{-1}) - y (n_{-1} \bar{u}_{-1})$$

It is noted that the right hand side of this equation is equal to the left hand side of Equation (5), and hence is  $\Phi$ , the optical invariant. Moreover both  $y$  values on the left apply to the surface to the left of the space, and both  $y$  values on the right refer to the surface to the right of the space. Therefore this equation shows that the optical invariant is also an invariant as the ray is transferred from one surface to the next.

6.3.5 The invariant for the entire system. We have shown above that there is a combination of  $y$ ,  $n$ ,  $u$ ,  $\bar{y}$ , and  $\bar{u}$ , which has the same value on either side of a surface, that is, it is invariant across a surface between two spaces. We have also shown that this same combination of parameters is the same on either

side of a space, that is, it is invariant across a space between two surfaces. Hence the optical invariant is an invariant for an entire optical system. It is therefore possible to write down the optical invariant between any two surfaces (or any two spaces). For example, between the object surface and the image surface we can write

$$\Phi = \bar{y}_o (n_o u_o) - y_o (n_o \bar{u}_o) = \bar{y}_k (n_{k-1} u_{k-1}) - y_k (n_{k-1} \bar{u}_{k-1}).$$

The invariant may also be written in determinant form as

$$\Phi = \begin{vmatrix} \bar{y} & n\bar{u} \\ y & nu \end{vmatrix}.$$

6.3.6 Lateral magnification. If  $y_o = 0$  on the object surface (the 0th surface), and  $y_k = 0$  on the image surface (the kth surface), then the next to the last equation becomes

$$\Phi = \bar{y}_o (n_o u_o) = \bar{y}_k (n_{k-1} u_{k-1}).$$

This is illustrated in Figure 6.2.

Using the optical invariant then, it is possible to calculate the height of the image  $\bar{y}_k$  from the object height,  $\bar{y}_o$ . The lateral magnification,  $m$ , is defined as

$$m = \frac{\bar{y}_k}{\bar{y}_o} = \frac{(n_o u_o)}{(n_{k-1} u_{k-1})}. \tag{7}$$

This equation shows that the lateral magnification can be calculated by tracing a single paraxial ray from the base of an object to the base of the image, and by taking the ratio given in Equation (7). Physically, the lateral magnification is the ratio of the height of the image to the height of the object, both heights being measured perpendicularly to the optical axis. By defining lateral magnification by Equation (7), and remembering that  $y$  values of points below the optical axis have signs opposite to those above, we see that a posi-

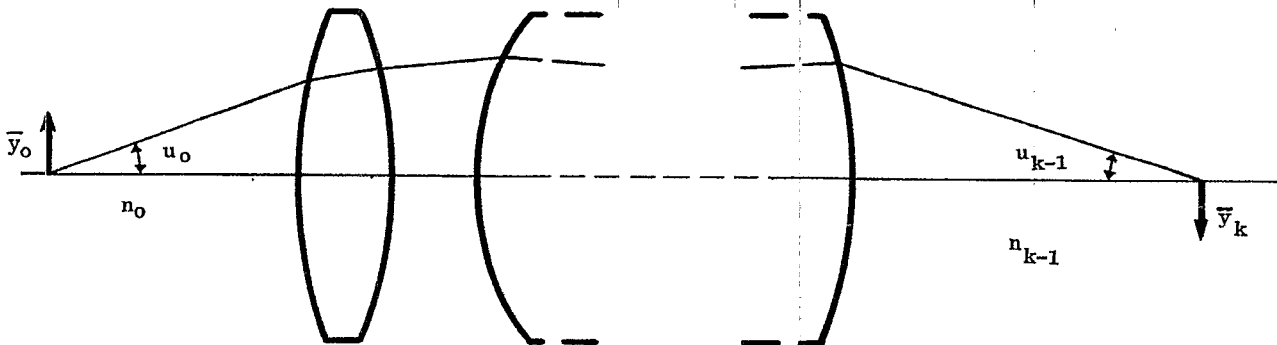


Figure 6.2 - Diagram illustrating the data used to compute the optical invariant.

tive value of  $m$  indicates an erect image. A negative value of  $m$  indicates an image inverted with respect to the object.

6.3.7 Angular magnification.

6.3.7.1 There are instruments which work with the object placed at a large distance  $t_o$  from the first surface of the lens or mirror. If this distance is great enough to assume it is infinite, then the ray coordinates on the first surface for the axial and oblique rays are:  $y_1$  ;  $u_o = 0$  ;  $\bar{y}_1$  ;  $\bar{u}_o$  . The optical invariant, for the first surface (1) and the space to the left (0), becomes

$$\Phi = - y_1 ( n_o \bar{u}_o ) .$$

In the image plane,  $y_k = 0$  , so

$$- y_1 ( n_o \bar{u}_o ) = \bar{y}_k ( n_{k-1} u_{k-1} ) ,$$

and

$$\bar{y}_k = \frac{- y_1}{( n_{k-1} u_{k-1} )} ( n_o \bar{u}_o ) . \tag{8}$$

In visual instruments, the image surface is usually at a great distance from the last optical surface (  $k - 1$  ). If the distance is assumed to be infinite, then  $u_{k-1} = 0$  , and

$$\Phi = - y_k ( n_{k-1} \bar{u}_{k-1} ) .$$

When both the object and image surfaces are assumed to be at infinity we have a telescopic system and the optical invariant is

$$\Phi = - y_1 ( n_o \bar{u}_o ) = - y_k ( n_{k-1} \bar{u}_{k-1} ) .$$

The most familiar example of a telescopic system is a telescope for which both object and image surfaces are at infinity; when so adjusted the telescope is said to be afocal. From the material to be presented in a

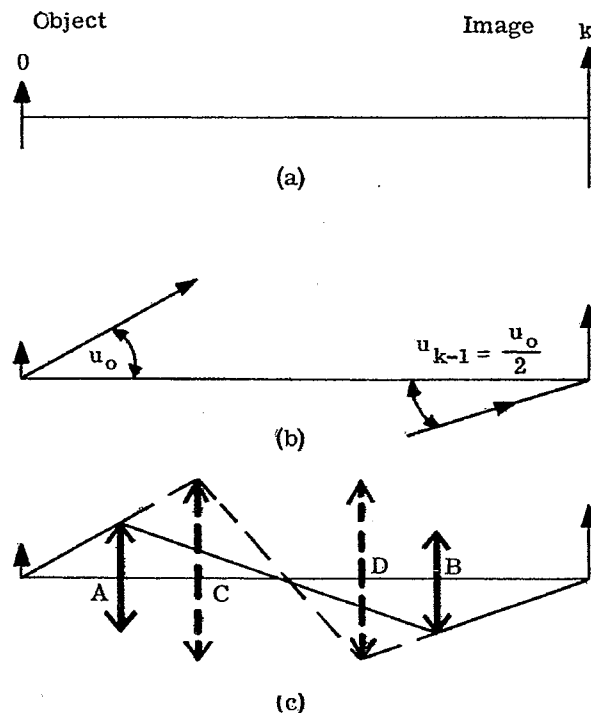


Figure 6.3 - Diagrams illustrating the use of the Smith Helmholtz equations. Thin positive lenses are represented by the symbol  $\downarrow$  , thin negative lenses by  $\uparrow$  .

later section we can say that such a telescope has its focal lengths equal to infinity and both focal points at infinity.

6.3.7.2 The angular magnification,  $\alpha$ , is defined as the ratio  $\bar{u}_{k-1}/\bar{u}_0$ . Therefore the angular magnification for a telescope in afocal adjustment is

$$\alpha = \frac{y_1 n_o}{y_k n_{k-1}} = MP. \quad (9)$$

For a telescope, the angular magnification is called the magnifying power (MP).

6.3.8 The Smith-Helmholtz and the Lagrange equations. Equations (7) and (8) can be rewritten as

$$\bar{y}_0 n_o u_o = \bar{y}_k n_{k-1} u_{k-1}$$

and

$$y_1 n_o \bar{u}_o = -\bar{y}_k n_{k-1} u_{k-1}.$$

These equations are referred to as the Smith-Helmholtz equations by some optical writers, and the LaGrange equations by others. Through the use of these equations, it is possible to decide rapidly what is needed to set up a given optical system. For example suppose we wish to form an erect image on surface  $k$  twice the size of the object on surface  $0$ . See Figure 6.3 (a). Equation (7) shows that if  $m$  is to be  $+2$  then  $u_o$  and  $u_{k-1}$  must have the same sign. This is illustrated in Figure 6.3 (b) for the case of  $n_o = n_{k-1}$ . A ray emerging from the base of the object at an angle  $u_o$  must pass through the optical system and emerge from below the optical axis at an angle  $u_o/2$ . As is shown in Figure 6.3 (c), this can be accomplished by any number of methods. A positive lens may be placed at  $A$  and be adjusted to refract the rays to cross the axis. At  $B$  a second positive lens refracts the rays to the final image. On the other hand two lenses could be used at  $C$  and  $D$  if desired, in which case the axial rays would refract as shown by the dotted lines.

## 6.4 LINEARITY OF THE PARAXIAL RAY TRACING EQUATIONS

6.4.1 General. In Sections 5.9.3 and 5.10 we have seen that finite heights and angles can be used with the paraxial ray trace equations. The basic reason for this is that these equations, 5-(56) and 5-(57), are linear. Another result of this linearity is that if two rays are traced through an optical system, it is possible to predict the path of any other paraxial ray. The proof of this fact will be developed below.

### 6.4.2 Proof of the theorem.

6.4.2.1 In order to prove the statements given above, let  $y$  and  $\bar{y}$  be the heights of any two paraxial rays on the  $j$ th surface. Corresponding to these two rays,  $u$  and  $\bar{u}$  are the angles between the rays and the optical axis. If  $\bar{y}$  and  $\bar{u}$  are the height and slope angle of any third ray, we wish to show that the equations

$$A \bar{y} + B y = \bar{y} \quad (10a)$$

and

$$A \bar{u} + B u = \bar{u} \quad (10b)$$

are valid for the entire optical system. We also must be able to calculate the values of  $A$  and  $B$ .

6.4.2.2 Equation (10a) applies to the  $j$ th surface. Using Equation 5-(56), we can show that an equation similar to (10a) applies to the  $j + 1$  surface. Substituting Equation 5-(56) into Equation (10a) gives

$$\bar{y}_{+1} - \frac{t}{n} (n\bar{u}) = A \bar{y}_{+1} - A \frac{t}{n} (n\bar{u}) + B y_{+1} - B \frac{t}{n} nu.$$

Collecting the terms involving  $n$  results in the expression  $t(\bar{u} - A\bar{u} - Bu)$ . But this equals zero by Equation (10b) so that

$$\bar{y}_{+1} = A \bar{y}_{+1} + B y_{+1}.$$

Hence Equation (10a) holds for the  $j + 1$  surface, and therefore, by induction, for any and all surfaces.



6.4.2.3 Similarly, we show that Equation (10b) holds for all spaces. Substituting Equation 5-(57) into Equation (10b), and collecting terms, we have

$$\frac{n_{+1}}{n} \bar{u}_{+1} = \frac{n_{+1}}{n} A \bar{u}_{+1} + \frac{n_{+1}}{n} B u_{+1} + \frac{c(n - n_{+1})}{n} (\bar{y} - A \bar{y} - B y).$$

By Equation (10a) the last term equals zero. Hence

$$\bar{u}_{+1} = A \bar{u}_{+1} + B u_{+1},$$

and Equation (10b) applies to any and all spaces.

6.4.2.4 We have shown that Equations (10a) and (10b) apply to all surfaces and all spaces respectively and hence to the entire optical system. Solving these equations for A and B gives

$$A = \frac{\bar{y} u - \bar{u} y}{\bar{y} u - \bar{u} y} = n (\bar{y} u - \bar{u} y) / \Phi$$

and

$$B = \frac{\bar{y} \bar{u} - \bar{u} \bar{y}}{\bar{y} u - \bar{u} y} = n (\bar{y} \bar{u} - \bar{u} \bar{y}) / \Phi.$$

These equations hold for any surface and the space to the right of that surface. In particular, we will use the expression for A for the object surface, and that for B for surface number 1.

6.4.3 Two particular rays.

6.4.3.1 Because the theorem proved in Section 6.4.2 holds for any three rays, we can choose these rays in

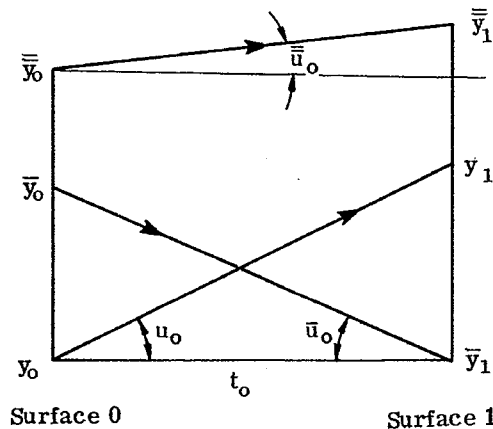


Figure 6.4 - Rays used to find simple expressions for A and B.

such a way as to simplify the calculation of A and B. The two particular rays we use are: (1) any ray from the center of the object surface ( $x_o = y_o = 0$ ), and (2) any ray from the object ( $\bar{y}_o \neq 0$ ) which intersects the axis at the center of the first surface ( $x_1 = \bar{y}_1 = 0$ ). These two particular rays, and any third ray, are shown in Figure 6.4. Using  $y_o = \bar{y}_1 = 0$ , the expressions for A and B reduce to

$$A = \bar{y}_o / \bar{y}_o ,$$

and

$$B = \bar{y}_1 / y_1 . \quad (11)$$

Using Figure 6.4, we have

$$y_1 = u_o t_o = -u_o \bar{y}_o / \bar{u}_o ,$$

and therefore

$$B = \frac{-\bar{y}_1 \bar{u}_o}{\bar{y}_o u_o} . \quad (12)$$

6.4.3.2 The two particular rays chosen are often specified more stringently. In order to get some idea as to the necessary diameters of the elements, the ray from the axial object ( $y_o = 0$ ) is taken at a value of  $u_o$  so as to pass through the edge of the aperture stop. Such a ray is called a rim ray, or marginal ray; the value of  $u_o$  determines the energy passing through the system. The other ray is taken as coming from the top of the object. This gives some idea as to the diameters of the elements necessary to attain the desired field of view. We will specify later that this second ray ( $\bar{y}_k \neq 0$ ) be the chief ray.

6.4.3.3 The above two paragraphs have specified the two particular rays ( $y_o = 0$  and  $\bar{y}_1 = 0$ ) be chosen so as to easily evaluate A and B from the known data and the initial third ray data. (It should be emphasized that this is not necessary; any two rays and the initial third ray data will suffice to determine A and B). Instead of choosing particular values of  $y_o$  and  $\bar{y}_1$ , we could have chosen particular values of  $u_o$  and  $\bar{u}_1$ , for example 0. This would result in  $A = \bar{u}_o / u_o$  and  $B = \bar{u}_1 / u_1$ . Note the correspondence between these and the equations in Paragraph 6.4.3.1.

## 6.5 THE CARDINAL POINTS OF AN OPTICAL SYSTEM

### 6.5.1 General.

6.5.1.1 We have already seen, in Sections 5.9.3, 5.10, and 6.4, some important consequences of the linearity of the paraxial ray trace equations. Another consequence, to be discussed in Section 6.5, is the presence of certain special points which exist in any optical system. Six of these points, all lying on the optical axis and known as the cardinal points, are of great usefulness in analyzing an optical system. The reason why the linearity of the paraxial ray equations lead to the existence of the cardinal points will not be developed in detail. It may be mentioned here, however, that the equations which we will develop from the concept of the cardinal points can be derived directly from the ray trace equations. One such equation, for example, was derived in Paragraph 6.2.3. The fact that both the paraxial ray equations and the assumption of the existence of cardinal points lead to the same equations is indicative of the connection between Sections 6.4 and 6.5.

6.5.1.2 The cardinal points, and the letters used to designate them, are as follows:

- (a) The first and second focal points,  $F_1$  and  $F_2$ .
- (b) The first and second principal points,  $P_1$  and  $P_2$ .
- (c) The first and second nodal points,  $N_1$  and  $N_2$ .

Sometimes the words first and second are replaced by primary and secondary, or by object and image, respectively.

6.5.2 The second focal point and the second focal length. In the sample calculation shown in Table 6.6, if the axial ray is traced from an infinitely distant object,  $t_o = \infty$  and  $u_o = 0$ . This ray will pass through the optical system and eventually cross the axis at what is called  $F_2$ , the second focal point. (See

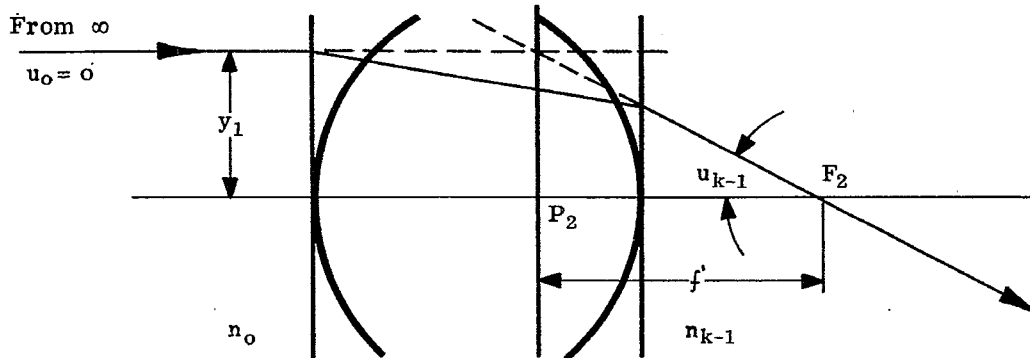


Figure 6.5 - Location of second focal point, second principal point, and second focal length.

Figure 6.5). The second focal point is, therefore, the intersection (in image space) of the optical axis and a ray which (in object space) was initially parallel to the optical axis. This cardinal point can also be considered as the axial image of an infinitely distant axial object. This is why it is sometimes referred to as the image focal point. Because the height of the axial ray,  $y_1$ , is arbitrary, all rays parallel to the optical axis, coming from an object surface, intersect at the second focal point. We can think of an image surface, intersecting the axis at  $F_2$ . This is the second focal surface, which for paraxial rays becomes the second focal plane. Then  $y_k = 0$ , and Equation (8) applies,

$$\bar{y}_k = -y_1 n_o \bar{u}_o / (n_{k-1} u_{k-1}) .$$

The second focal length is defined as,

$$f' = -y_1 / u_{k-1} . \tag{13}$$

Physically, the second focal length is the distance between the second focal point and the second principal point, defined below. The reason a telescope in afocal adjustment (see Paragraph 6.3.7.1) has an infinite (second) focal length is that  $u_{k-1} = 0$ . Hence the final axial ray is parallel to the axis, and  $F_2$  is at infinity.

6.5.3 The second principal point. The second principal point is located by erecting a plane perpendicular to the optical axis at the point of intersection of the forward-extended entering ray and the backward-extended exit ray. The intersection of this plane (the second principal plane) with the optical axis is the second principal point,  $P_2$ . From Figure 6.5 it can be seen that

$$f' = P_2 F_2 .$$

If the second principal point is to the left of the second focal point,  $f'$  is positive; otherwise it is negative.

6.5.4 The second nodal point. The second nodal point,  $N_2$ , is also an axial point, as are  $F_2$  and  $P_2$ . It is a point such that the distance

$$N_2 F_2 = (P_2 F_2) \frac{n_o}{n_{k-1}} .$$

With this expression Equation (8) can then be written

$$\bar{y}_k = f' \frac{n_o \bar{u}_o}{n_{k-1}} = P_2 F_2 \frac{n_o \bar{u}_o}{n_{k-1}} = N_2 F_2 \bar{u}_o .$$

If  $n_o = n_{k-1}$ , then  $P_2 F_2$  and  $N_2 F_2$  are equal and the principal point  $P_2$  and the nodal point  $N_2$  coincide.

6.5.5 The first focal, principal and nodal points.

6.5.5.1 With similar arguments one can find a first focal point,  $F_1$ , such that rays entering the system from  $F_1$  will emerge from the last surface traveling parallel to the axis. For such an object point,  $y_o = 0$ , and  $u_{k-1} = 0$ . Therefore from the optical invariant equation,

$$\bar{y}_o = - y_k \frac{n_{k-1} \bar{u}_{k-1}}{n_o u_o} .$$

The first focal length  $f$  is now defined as,

$$f = \frac{y_k}{u_o} = F_1 P_1 . \tag{14}$$

Finally using  $F_1 N_1 = (F_1 P_1) \frac{n_{k-1}}{n_o}$ , we have

$$\bar{y}_o = - f \frac{n_{k-1} \bar{u}_{k-1}}{n_o} = - F_1 P_1 \frac{n_{k-1} \bar{u}_{k-1}}{n_o} = - F_1 N_1 \bar{u}_{k-1} .$$

6.5.5.2 The physical meanings of the first focal and principal points, and the first focal length, correspond to those discussed in Sections 6.5.2 and 6.5.3. The first focal point (see Figure 6.6) is the intersection of the optical axis and a ray which will be parallel to the axis when it leaves the system. It is also the axial object whose axial image is infinitely distant. All rays parallel to the optical axis after emerging from the

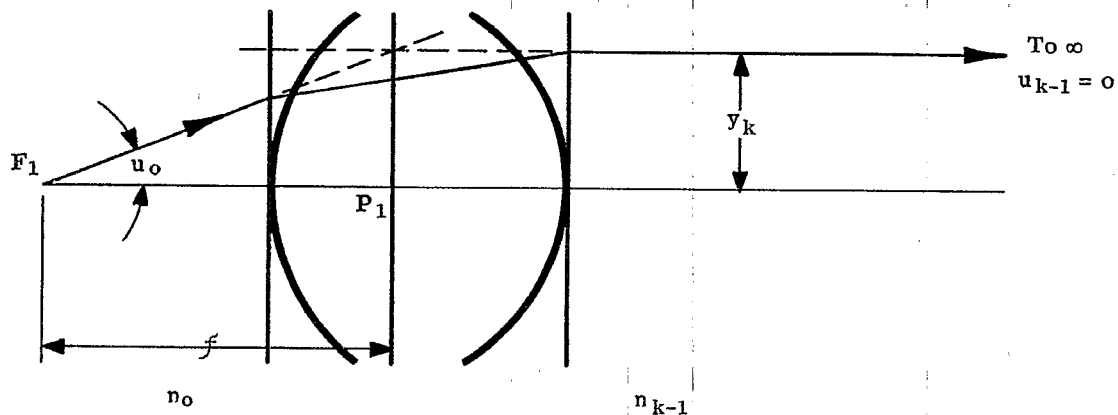


Figure 6.6 - Location of first focal point, first principal point, and first focal length.

system have passed through the first focal point. The plane perpendicular to the axis at  $F_1$  is the first focal plane.

6.5.5.3 The first principal plane is a plane perpendicular to the optical axis passing through the intersection of the forward-extended ray through  $F_1$  and the backward-extended ray emerging from the system parallel to the axis. The intersection of this plane with the axis is the first principal point. The first focal length is the distance between the first focal point and the first principal point, and is positive if  $F_1$  lies to the left of  $P_1$ .

#### 6.5.6 Object and image positions with respect to focal and principal points.

6.5.6.1 The previous sections, in connection with Figures 6.5 and 6.6, have explained the meaning of the focal and principal points, and the principal planes, from a graphical point of view. First, these ideas will be used to derive some well known relations between object and image positions. These relations will then be used to indicate additional characteristics of principal planes and nodal points.

6.5.6.2 Consider Figure 6.7 which indicates an object of height  $\bar{y}_o$  at an arbitrary position. It should be emphasized here that Figure 6.7 indicates a general optical system, without reference to specific positions of refracting or reflecting surfaces. (Figures 6.5 and 6.6 show two refracting surfaces merely for concreteness; the ideas involved in those figures apply to the general system, as does the whole of Section 6.5). Of the infinite number of rays that come from the top of the object, we choose two whose course through the system we know from Figures 6.5 and 6.6. An entering ray, parallel to the optical axis, passes through  $F_2$ , and can be considered to be deviated only once, at the second principal plane. Similarly, a ray through  $F_1$  exits parallel to the optical axis, and can be considered as having been deviated only once, at the first principal plane.

6.5.6.3 Four new distances are shown,  $Z$ ,  $Z'$ ,  $S$ , and  $S'$ . Sign conventions are then established such that all these distances shown, as well as  $f$  and  $f'$ , are positive. If any pair of points at the ends of the double arrows are reversed, the distance is negative. For example if the object is to the right of  $F_1$ ,  $Z$

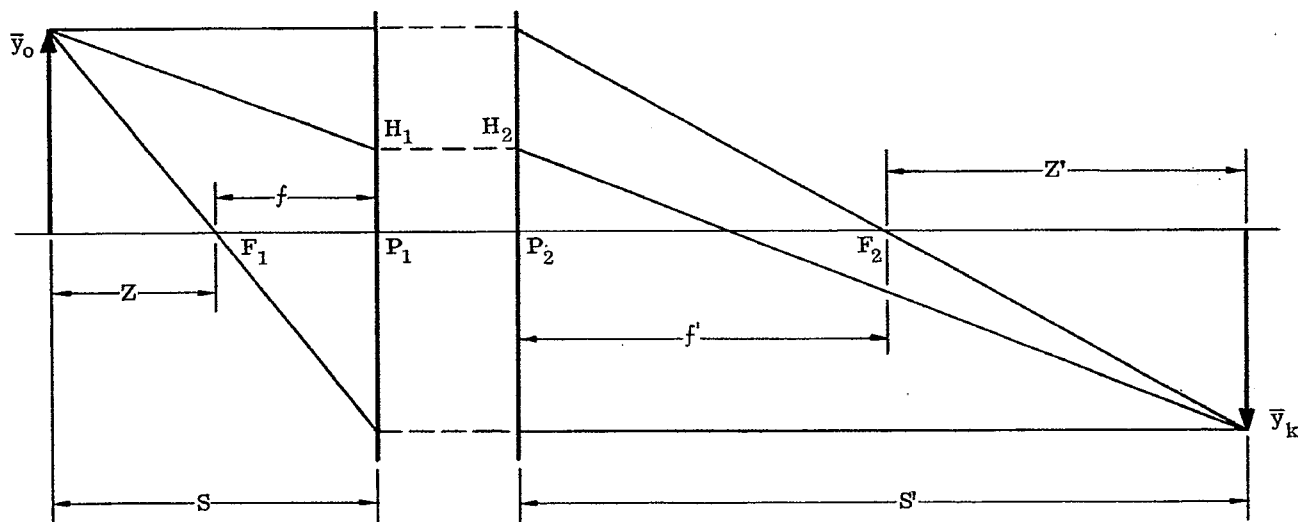


Figure 6.7 - Diagram showing object and image relations.

will be negative. From similar triangles, remembering that  $\bar{y}_k$  is negative,

$$\frac{\bar{y}_k}{\bar{y}_o} = -\frac{Z'}{f'} = -\frac{f}{Z}.$$

Using the definition of lateral magnification,  $m = \bar{y}_k / \bar{y}_o$ , we have

$$m = -\frac{Z'}{f'} = -\frac{f}{Z}. \quad (15)$$

Rearranging there follows

$$ZZ' = ff'. \quad (16)$$

Equations (15) and (16) are in the Newtonian form, in which object and image positions are measured from the focal points,  $F_1$  and  $F_2$ , respectively.

6.5.6.4 Another form of expressing these relations is the Gaussian form of these equations, in which object and image positions are measured from the principal points,  $P_1$  and  $P_2$ , respectively. From Figure 6.7,  $Z = S - f$  and  $Z' = S' - f'$ . Substituting these expressions into (15) and (16) gives

$$m = -\frac{S' - f'}{f'} = -\frac{f}{S - f}$$

and

$$(S - f)(S' - f') = ff'.$$

Expanding the last equation and dividing by  $SS'$ , we have

$$\frac{f}{S} + \frac{f'}{S'} = 1, \quad (17)$$

and using (17), the lateral magnification becomes

$$m = -\frac{fS'}{f'S}. \quad (18)$$

Equations (18) and (17) are in the Gaussian form and correspond to Equations (15) and (16). Whereas the latter pair does not involve  $S$  or  $S'$ , and the former pair does not involve  $Z$  or  $Z'$ , we may eliminate  $f$  and  $f'$  from Equation (16) by substituting  $f = S - Z$  and  $f' = S' - Z'$ . The result is

$$\frac{Z}{S} + \frac{Z'}{S'} = 1.$$

And using this with Equation (15), we have

$$m = -\frac{Z'S}{ZS'}.$$

6.5.6.5 It may be well to summarize here the specific meanings of the six distances used in the equations of Paragraphs 6.5.6.3 and 6.5.6.4. The sign conventions are included below if it is remembered that a distance measured to the right is positive.

- $f$  is measured from  $F_1$  to  $P_1$ .
- $f'$  is measured from  $P_2$  to  $F_2$ .
- $Z$  is measured from the object plane to  $F_1$ .
- $Z'$  is measured from  $F_2$  to the image plane.
- $S$  is measured from the object plane to  $P_1$ .
- $S'$  is measured from  $P_2$  to the image plane.

6.5.7 Additional characteristics of principal planes. Suppose the object is placed at the first principal plane. This means that  $Z = -f$ , and Equation (16) gives  $Z' = -f'$ . But this also means that the image is at the second principal plane; the two principal planes are therefore conjugate planes and  $P_1$  and  $P_2$  are conjugate points. (Equation (17) could have been used, with  $S = 0$ , giving  $S' = 0$ , which again locates the image at  $P_2$ ). Using Equation (15) we find for this case  $m = 1$ . The two principal planes are therefore planes of unit positive magnification. This fact is very useful since it allows us to say that any point on the plane through  $P_1$  is imaged at the same height on the plane through  $P_2$ . Therefore any other ray (see Figure 6.7), entering the system so that it intersects the first principal plane at  $H_1$ , exits from the system as if it came from  $H_2$ , at the same distance from the axis.

6.5.8 Additional characteristics of nodal points.

6.5.8.1 There is an important relation between the focal lengths of any optical system, and the refractive indices of object and image space. Equation (7) can be rewritten, using Figure 6.7, to give

$$m = \frac{n_o u_o}{n_{k-1} u_{k-1}} = \frac{n_o}{n_{k-1}} \left( -\frac{S'}{S} \right).$$

Comparing this with Equation (18) we have

$$f/n_o = f'/n_{k-1} . \tag{19}$$

6.5.8.2 Equation (19) can be used to indicate a useful property of the nodal points. Using the expressions for  $N_2 F_2$  and  $F_1 N_1$  given in Sections 6.5.4 and 6.5.5, in connection with Figure 6.8, we have

$$P_1 N_1 = F_1 N_1 - F_1 P_1 = f \left( \frac{n_{k-1}}{n_o} - 1 \right) = \frac{f}{n_o} (n_{k-1} - n_o),$$

and

$$P_2 N_2 = P_2 F_2 - N_2 F_2 = f' \left( 1 - \frac{n_o}{n_{k-1}} \right) = \frac{f'}{n_{k-1}} (n_{k-1} - n_o).$$

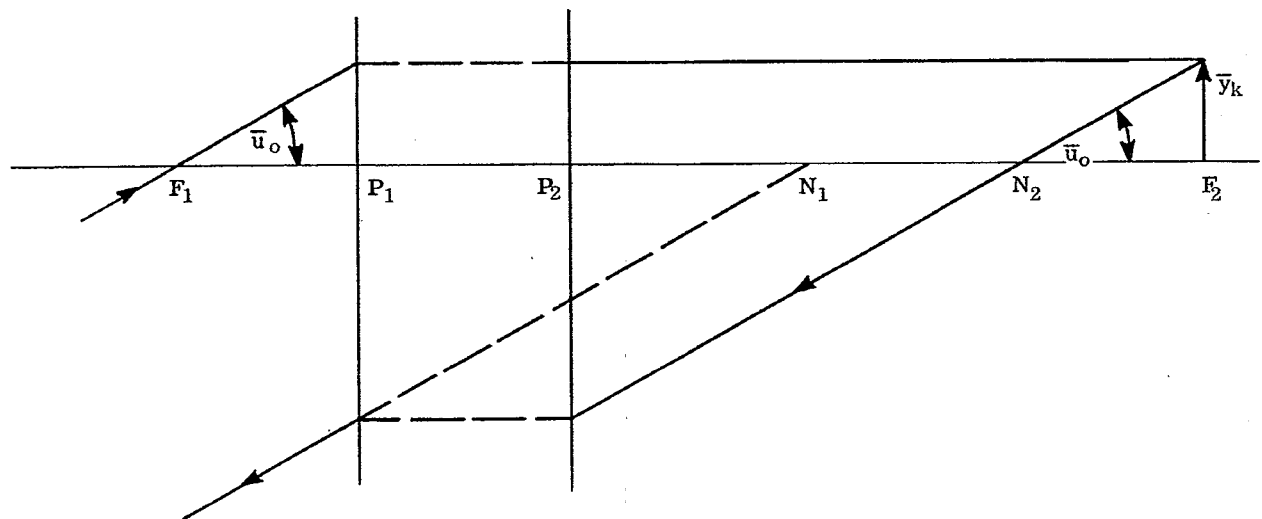


Figure 6.8 - Graphical construction to locate positions of nodal points.

Because of Equation (19), the following relations hold between the cardinal points.

$$P_1 N_1 = P_2 N_2 ,$$

$$P_1 P_2 = N_1 N_2 ,$$

$$F_1 N_1 = f' ,$$

$$N_2 F_2 = f .$$

And for object and image media the same,  $n_o = n_{k-1}$ ,  $f = f'$ , and the principal and nodal points coincide,  $P_1$  with  $N_1$ , and  $P_2$  with  $N_2$ .

6.5.8.3 Because  $P_1 P_2 = N_1 N_2$ , two parallel lines, one through each nodal point, will intersect the principal planes in points equidistant from the axis. Hence these two rays are conjugate rays, and we have the important fact that any ray in object space which is heading toward  $N_1$  will emerge from the system in the same direction from  $N_2$ . This gives us a graphical method for locating the nodal points, shown in Figure 6.8. A ray is shown entering the system at an angle  $\bar{u}_o$  headed towards  $F_1$  until it intersects the plane at  $P_1$ . It then emerges from the plane at  $P_2$  parallel to the axis at the image height  $\bar{y}_k$ . A ray then traced backwards at an angle  $\bar{u}_o$  with the axis must emerge anti-parallel to the entering ray as shown in the illustration, because all rays leaving a point on the focal plane are parallel to each other after emerging from the system. The two points  $N_1$  and  $N_2$  are the intersections with the axis of the two segments of this backwards traced ray.

6.5.9 Numerical example. A numerical example, represented in Figure 6.9, shows the location of the cardinal points of a lens with water on one side and air on the other. Given the three indices, two curvatures, and lens thickness, all other numerical values can be found using the equations already developed. An axial ray is traced through the system at  $u_o = 0$  and  $y_1$  arbitrary.  $t_2$  can be found, using  $y_3 = 0$ . Therefore  $F_2$  is located with respect to the second surface of the lens. A corresponding trace locates  $F_1$ . Equations (13) and (19) give  $f'$  and  $f$  respectively. The principal points and nodal points can now be located.

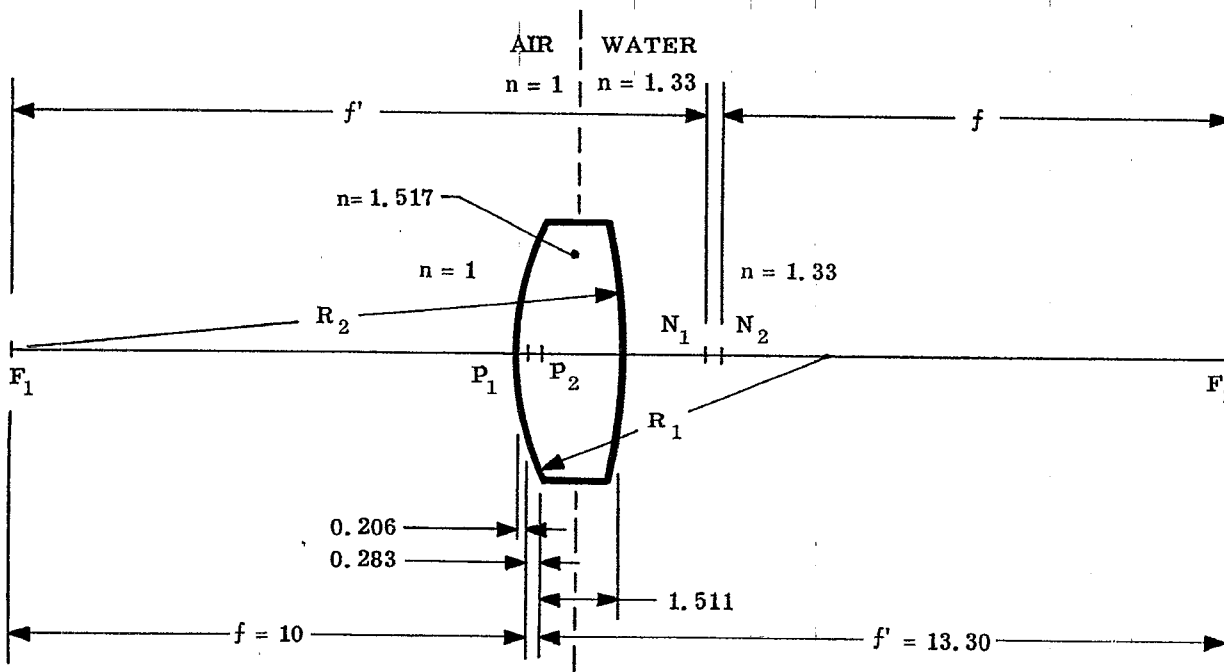


Figure 6.9- Numerical example showing location of the cardinal points for a lens with water on one side.



## 6.6 CALCULATION OF THE FOCAL LENGTH FROM FINITE CONJUGATE DATA

6.6.1 General. If an optical system is to be used at infinite conjugate, that is either the object or image or both are at infinity, then the entering axial ray is traced at  $u_o = 0$ ,  $y_1$  arbitrary. (For systems having the image at infinity for a finite object, the design is considered as if the rays went backwards through the system. Systems are therefore designed with the infinite conjugate as object, whether or not this agrees with the physical situation. The justification for this is that an optical system is reversible in the sense that rays traverse the same path in either direction). The ray trace automatically gives the focal length,  $f'$ , by using Equation (13).

6.6.2 Finite conjugates. However, if the system images a finite conjugate object, and an axial ray and an oblique paraxial have been traced, Equation (13) does not apply. It is possible, nevertheless, from the data obtained from these two rays, to calculate the focal length. If two rays have been traced as shown in Figure 6.4 and in the presentation of Table 6.6, then

$$A = \bar{y}_o / \bar{y}_o$$

and

$$B = -\bar{y}_1 \bar{u}_o / \bar{y}_o u_o, \text{ this latter being Equation (12).}$$

With these constants known, it is possible to predict the final  $\bar{u}_{k-1}$  for a ray entering the lens parallel to the axis. For then  $\bar{u}_o = 0$  and  $\bar{y}_o (= \bar{y}_1)$  are the initial conditions for the third ray.

Now writing Equation (10b) for the final angle,

$$\bar{u}_{k-1} = \frac{\bar{y}_o}{y_o} \bar{u}_{k-1} - \frac{\bar{y}_1 \bar{u}_o}{y_o u_o} u_{k-1}$$

From this equation, and Equation (13) written for the third ray, we have

$$f' = - \frac{\Phi}{n_o (u_o \bar{u}_{k-1} - \bar{u}_o u_{k-1})} \quad (20)$$

where  $\Phi = \bar{y}_o (n_o u_o)$  from Paragraph 6.3.6.

## 6.7 SYSTEMS OF THIN LENSES IN AIR

6.7.1 Concept of the thin lens.

6.7.1.1 None of the basic material presented so far presupposes any specific form of the optical system other than that it is a centered system. We now want to specialize the system somewhat and consider a single lens, an example of which is shown in Figure 6.9. In that example,  $n_o \neq n_2$ , so that  $f \neq f'$ . If  $n_o = n_2 = 1$ , the lens is in air, and  $f = f'$ . The nodal and principal points coincide as explained in Paragraph 6.5.8.2. Because of the equality of the two focal lengths, Equations (15) through (18) can be simplified.

6.7.1.2 An additional simplification can be attained by assuming that the axial lens thickness,  $t_1$  in the above example, is small compared with  $t_o$  and  $t_2$ . If  $t_1$  can be neglected, the lens is called a thin lens. Since the two deviations of the ray are considered to occur at one point, for a thin lens, both principal planes coincide with the lens of zero thickness. For this case,  $S$  and  $S'$  are the distances measured to the intersection of the lens with the optical axis, and Equations (17) and (18) take the familiar form for a thin lens in air. The two nodal points also coincide with the lens; hence a ray directed towards the lens center will emerge from the same point in the same direction. In some special cases, such as high curvature meniscus lenses (highly warped lenses), the thickness may be small, but not completely negligible. In these cases the lens may be "thin" for certain applications (for example, calculation of focal length), but not "thin" for others (for example, calculation of principal points positions). In such intermediate cases, where the lens is neither completely thick or completely thin, the principal and nodal points do not necessarily coincide with the center of the lens.

6.7.2 Focal length and power of a thin lens in air. Many optical systems are made up of individual two-surface lenses separated by air. Paraxial rays can, of course, be traced through any system of this type by using Equations 5-(56) and 5-(57), but considerable simplification can be made if it can be assumed that the individual lenses are thin. In the layout shown in Table 6.8, an axial paraxial ray and an oblique paraxial

ray are traced through a thin, two-surface element in air. For the axial paraxial ray, we have

$$u_o = y/t_o ,$$

$$u_2 = y/t_o + y(1-n)c_1 + y(n-1)c_2 ,$$

and

$$u_2 = u_o - y(n-1)(c_1 - c_2) . \tag{21}$$

The focal length may be calculated from Equation (20), using  $\Phi = \bar{y}_o (n_o u_o)$ . If numerical calculations are made, the data are found in a table similar to Table 6.8. Therefore,

$$f' = - \frac{\Phi}{n_o (\bar{u}_2 u_o - \bar{u}_o u_2)} = \frac{t_o \bar{u}_o u_o}{(\bar{u}_o u_o - \bar{u}_o u_2)} ,$$

or

$$f' = \frac{t_o u_o}{u_o - u_2} = \frac{1}{(n-1)(c_1 - c_2)}$$

and

$$1/f' = (n-1)(c_1 - c_2) = \phi . \tag{22}$$

Equation (22) is the well known formula for the focal length of a thin lens in air. It is more convenient to use it in the latter form, where  $\phi$  is called the power of the thin lens.

| SURFACE      | Object           | 1                   | 2                               | 3     |
|--------------|------------------|---------------------|---------------------------------|-------|
| c            | $c_o$            | $c_1$               | $c_2$                           | $c_3$ |
| t            | $t_o$            | 0                   | $t_2$                           |       |
| n            | 1                | n                   | 1                               |       |
| $(n_1 - n)c$ | 0                | $(1-n)c_1$          | $(n-1)c_2$                      |       |
| $t/n$        | $t_o$            | 0                   | $t_2$                           |       |
| y            | 0                | y                   | y                               | 0     |
| nu           | $y/t_o$          | $y(1-n)c_1 + y/t_o$ | $y(n-1)c_2 + y(1-n)c_1 + y/t_o$ |       |
| $\bar{y}$    | $-t_o \bar{u}_o$ | 0                   | 0                               |       |
| $n\bar{u}$   | $\bar{u}_o$      | $\bar{u}_1$         | $\bar{u}_2$                     |       |

$$\bar{u}_o = \bar{u}_1 = \bar{u}_2$$

Table 6.8- Paraxial rays traced through a thin lens.

6.7.3 Ray trace equations for thin lens systems in air.

6.7.3.1 Equation (21) can be written

$$u_2 = u_o - y \phi .$$

The similarity between this and Equation 5-(57) is now apparent. Equation 5-(56) can be used to transfer between lenses. We have then the transfer and refraction equations for thin lens systems. These equations, (23) and (24), are written for a general thin lens j.

$$y = y_{-1} + t_{-1} u_{-1} , \tag{23}$$

$$u = u_{-1} + y (-\phi) . \tag{24}$$

Table 6.9 illustrates a method using Equations (23) and (24) for calculating the familiar expression for the

focal length of a dialyte, i.e., two thin lenses separated by the distance  $d$ .

| SURFACE        | LENS (a)   | LENS (b)                          | IMAGE                                   |
|----------------|------------|-----------------------------------|---|
| $-\phi$<br>$d$ | $-\phi a$  | $-\phi b$                         |   |
| $y$<br>$u$     | $y_1$<br>0 | $(1-d\phi a)y_1$<br>$-\phi a y_1$ | $(-\phi a - \phi b + d\phi a\phi b)y_1$ |

$$\frac{1}{f'} = \phi = - \frac{u_{k-1}}{y_1} = \phi a + \phi b - d \phi a \phi b$$

Table 6.9 - Tracing a paraxial ray,  $u_o = 0$  and  $y_1$  arbitrary through two thin lenses.

6.7.3.2 The tracing of paraxial rays through thin lens systems is probably the one remaining calculation that lens designers do on desk calculators. In optical design work, a great deal of time and thought must necessarily go into the preliminary layout work. The designer must decide where to place the lenses, and what focal lengths are to be used. He needs to know approximately the sizes of lenses needed, and the approximate path of rays as they pass through the system. All these calculations can be made assuming thin lenses, and it is a problem so varied that it does not lend itself well to a large computer. Experience shows that desk calculators or slide rules are preferred at this stage of the design.

6.8 OPTICAL SYSTEMS INVOLVING MIRRORS

6.8.1 Sign conventions. It was pointed out in Section 2.3.3 that the equation of refraction could be used for reflection by merely writing

$$n_{+1} = - n .$$

If this is done in all the refraction equations, they can be used for reflection. If a mirror is inserted in an optical system, it reflects the ray backwards so that if the light was originally traveling from left to right, it will travel from right to left after reflection. It is possible to treat reflecting surfaces in exactly the same way as refraction surfaces by adopting the following rules:

- (1) Write all the curvatures with the usual sign convention. If a single surface is encountered several times in a reflecting system, the radius is always considered to have the same sign.
- (2) Whenever the light travels from right to left, insert the index and thickness with a negative sign.

6.8.2 A mirror system and its ray tracing format. A typical mirror and lens system is shown in Figure 6.10. The proper way to lay out the data for ray tracing is shown in Table 6.10. Actual rays as well as paraxial rays can then be traced through this system exactly as though it were only a refracting lens. If the light travels from right to left in the  $j$ th space one must remember that the index of refraction ( $n_j$ ) is negative.

6.8.3 First order imagery in a mirror.

6.8.3.1 By using the above procedure it is now possible to readily work out the first order optics of a single mirror. The problem is illustrated in Figure 6.11, and worked out in the presentation shown in Table 6.11. From the table, it is apparent, by applying Equation 5-(56), that

$$y_2 = 0 = 1 + (-t_1) \left( \frac{1}{t_o} + 2c \right) .$$

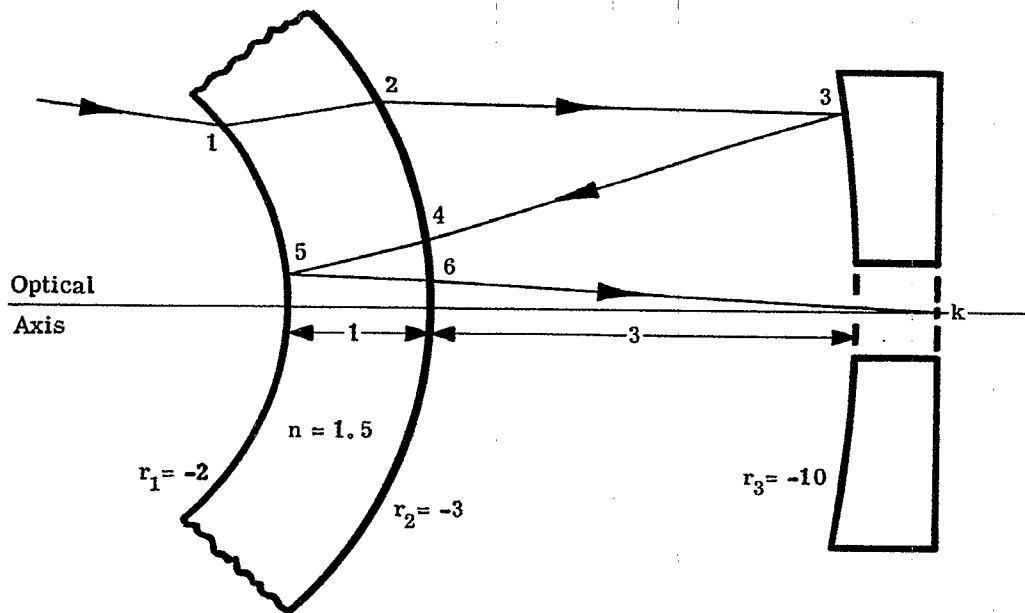


Figure 6.10 - The path of rays through a mirror system.

| SURFACE         | OBJECT   | 1      | 2      | 3      | 4      | 5      | 6      | k |
|-----------------|----------|--------|--------|--------|--------|--------|--------|---|
| c               | 0        | -0.500 | -0.330 | -0.100 | -0.330 | -0.500 | -0.330 | 0 |
| t               | $\infty$ | 1.000  | 3.000  | -3.000 | -1.000 | 1.000  | 1.000  |   |
| n               | 1.000    | 1.500  | 1.000  | -1.000 | -1.500 | 1.500  | 1.000  |   |
| $c(n_{-1} - n)$ | 0        | 0.250  | -0.165 | -0.200 | -0.165 | 1.500  | -0.165 | 0 |
| t/n             | $\infty$ | 0.667  | 3.000  | 3.000  | 0.667  | 0.667  |        |   |

Table 6.10 - Computing sheet format for mirror system illustrated above. Only the lens constants are included in the above table. The calculations, which are not given, are carried out as in Table 6.6.

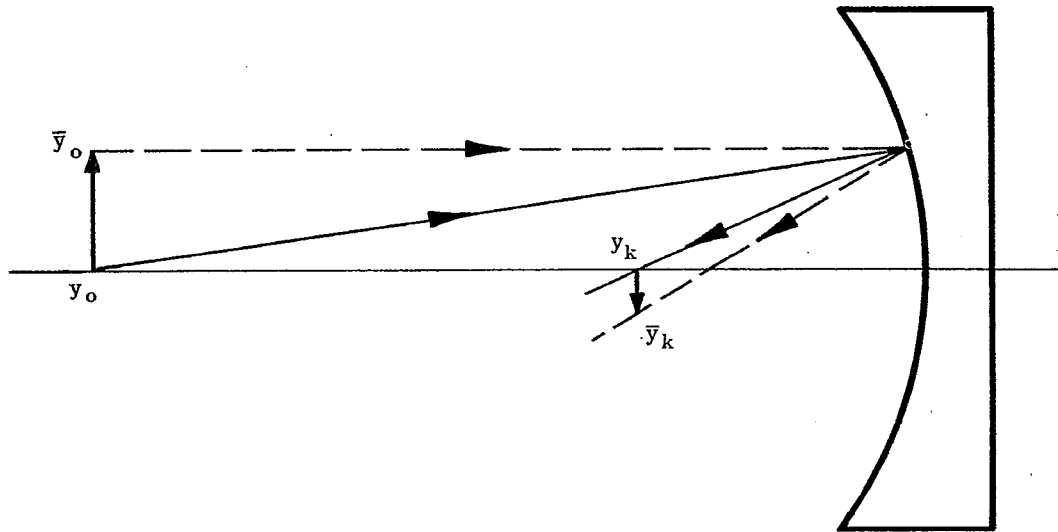


Figure 6.11 - Imaging an object in a concave mirror.

| SURFACE         | OBJECT | 1       | IMAGE        |
|-----------------|--------|---------|--------------|
| $c$             | 0      | $c$     | 0            |
| $t$             |        | $t_o$   | $t_1$        |
| $n$             |        | 1       | -1           |
| $c(n_{-1} - n)$ | 0      | $2c$    | 0            |
| $t/n$           |        | $t_o$   | $-t_1$       |
| $y$             | 0      | 1       | 0            |
| $nu$            |        | $1/t_o$ | $1/t_o + 2c$ |
| $\bar{y}$       | 1      | 1       | $1 - t_1 2c$ |
| $n\bar{u}$ *    |        | 0       | $2c$         |

\* Ray traced parallel to axis to calculate focal length directly.

Table 6.11 - Ray tracing through a single mirror system.

Therefore

$$\frac{1}{t_1} = \frac{1}{t_o} + 2c = \frac{1}{t_o} + \frac{2}{r} \tag{25}$$

For a numerical example assume  $r = -10$  and  $t_o = 20$ . Then  $t_1 = -20/3$ . The minus sign indicates that the image surface lies to the left of the mirror surface, as shown in Figure 6.11. The same equation could have been derived using Equation (1),

$$\frac{n_1}{t_1} + \frac{n_o}{t_o} = c_1 (n_1 - n_o)$$

and setting

$$n_1 = -n_o$$

The magnification for the mirror may be found from Equation (7),

$$m = \frac{n_o u_o}{n_1 u_1} = \frac{1/t_o}{(1/t_o) + 2c} = t_1 / t_o$$

The same equation could have been derived from Equation (18), remembering that  $f' = -f$  because  $n_1 = -n_o$ .

6.8.3.2 The focal length of the mirror may be found by tracing a paraxial ray through the mirror at  $\bar{y}_1 = 1$  and  $\bar{u}_o = 0$  as noted in the lower two lines in Table 6.11. Equation (13) can be written

$$f' = - \frac{y_1 n_{k-1}}{(n_{k-1} u_{k-1})}$$

and used with the ray at  $\bar{u}_o = 0$ .

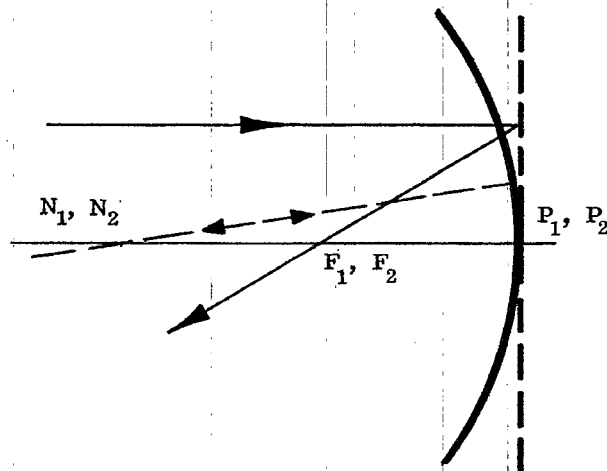


Figure 6.12 - The location of the principal points, focal points, and nodal points for a single mirror system.

Since  $n_0 = -n_{k-1}$ ,  $\bar{y}_1 = 1$ , and  $(n_{k-1} \bar{u}_{k-1}) = 2c$ , we have,

$$f' = \frac{n_0}{2c} = n_0 \frac{r}{2}.$$

If  $r$  is negative as it is in Figure 6.11,  $f'$  is negative indicating that  $F_2$  lies to the left of  $P_2$ . The equation  $P_2 F_2 n_0 = n_{k-1} N_2 F_2$  shows that for the mirror,

$$P_2 F_2 = -N_2 F_2.$$

Since  $P_2 F_2$  is negative for the example shown in Figure 6.11, then  $N_2 F_2$  is positive. The location of  $P_1, N_1, F_1, P_2, N_2$  and  $F_2$  are shown in Figure 6.12. The nodal points are at the center of curvature.

## 6.9 DIFFERENTIAL CHANGES IN FIRST ORDER OPTICS

### 6.9.1 General.

6.9.1.1 The various steps followed in the design of an optical system are discussed in Section 9. The first two steps of the procedure are (1) selection of type of element for each part of the system, and (2) calculation of a first order thin lens solution. Step (2) involves the calculation of the focal lengths and separations of the individual elements, as well as first order aberrations which will be discussed in Section 6.10. The basic procedure for tracing paraxial rays, and therefore for determining focal lengths and spacings, have already been outlined in Section 6.

6.9.1.2 After the completion of step (2) the designer may feel that some changes are necessary so that the system meets more closely the required specifications. For example, he may have to change the focal length of the system. At the present stage of the system design (thin lens, paraxial rays), the designer can vary only the curvatures, the separations, and the indices of refraction. It therefore becomes important to know how changes in these three parameters affect the first order solution. In the remainder of Section 6.9 formulae will be given for computing the effects on first order optics for differential changes in the lens parameters.

### 6.9.2 Determination of the differential coefficients.

6.9.2.1 A change of any parameter, such as thickness, index of refraction, or curvature of a surface, will result in the paraxial ray changing its path to the next surface. Specifically, changes in  $t$  will change  $y_{+1}$ , and changes in  $n$  or  $c$  will change both  $u$  and  $y_{+1}$ . These changes will, in turn, cause changes on each surface up to and including the final image. The final changes,  $dy_k$  and  $du_{k-1}$ , which result from a change of any parameter associated with the  $j$ th surface, is certainly a function of changes  $dy_{j+1}$  and  $du_j$ . If the changes can be assumed to be differentials, it is possible to write

$$dy_k = \left( \frac{\partial y_k}{\partial y_{+1}} \right) dy_{+1} + \left( \frac{\partial y_k}{\partial u} \right) du \quad (26)$$

and

$$du_{k-1} = \left( \frac{\partial u_{k-1}}{\partial y_{+1}} \right) dy_{+1} + \left( \frac{\partial u_{k-1}}{\partial u} \right) du. \quad (27)$$

6.9.2.2 The partial derivatives in the above equations are called differential coefficients. If we trace two differential rays through the system, we have two values each for  $\bar{y}_{+1}$  and  $\bar{u}$  (initial ray data) and two values each for  $dy_k$  and  $du_{k-1}$  (result of ray trace). Therefore, by tracing two differential rays near a given ray, it should be possible to determine the respective differential coefficients. It was shown in Section 5.9 that a paraxial ray is a differential ray traced near the optical axis. Therefore, we will use the axial paraxial ray and the oblique paraxial ray as the two differentially traced rays near the optical axis, taken as the given ray. It is possible then to evaluate the differential coefficients for changes in  $y_k$  and  $u_{k-1}$ , by making the following substitutions in Equations (26) and (27):

$$\begin{array}{llll} dy_k = y_k & dy_{+1} = y_{+1} & du = u & du_{k-1} = u_{k-1} \\ d\bar{y}_k = \bar{y}_k & d\bar{y}_{+1} = \bar{y}_{+1} & d\bar{u} = \bar{u} & d\bar{u}_{k-1} = \bar{u}_{k-1} \end{array}$$

Two sets of simultaneous equations are thereby obtained. These equations, when solved for the derivatives, give:

$$\frac{\partial y_k}{\partial y_{+1}} = \frac{(\bar{y}_k u - y_k \bar{u})}{(\bar{y}_{+1} u - y_{+1} \bar{u})} = \frac{n(\bar{y}_k u - y_k \bar{u})}{\Phi}, \quad (28)$$

$$\frac{\partial y_k}{\partial u} = \frac{(y_k \bar{y}_{+1} - \bar{y}_k y_{+1})}{(\bar{y}_{+1} u - y_{+1} \bar{u})} = \frac{n(y_k \bar{y}_{+1} - \bar{y}_k y_{+1})}{\Phi}, \quad (29)$$

$$\frac{\partial u_{k-1}}{\partial y_{+1}} = \frac{(\bar{u}_{k-1} u - u_{k-1} \bar{u})}{(\bar{y}_{+1} u - y_{+1} \bar{u})} = \frac{n(\bar{u}_{k-1} u - u_{k-1} \bar{u})}{\Phi}, \quad (30)$$

and

$$\frac{\partial u_{k-1}}{\partial u} = \frac{(\bar{y}_{+1} u_{k-1} - y_{+1} \bar{u}_{k-1})}{(\bar{y}_{+1} u - y_{+1} \bar{u})} = \frac{n(\bar{y}_{+1} u_{k-1} - y_{+1} \bar{u}_{k-1})}{\Phi}. \quad (31)$$

### 6.9.3 Effect of curvature change on focal length.

6.9.3.1 The change in focal length,  $df'$ , due to changes in curvature, thickness, and index is given by

$$df' = \left( \frac{\partial f'}{\partial c} \right) dc + \left( \frac{\partial f'}{\partial t} \right) dt + \left( \frac{\partial f'}{\partial n} \right) dn.$$

If the differential coefficients are known, then  $df'$  can be found for any small change in the system parameters. It will now be assumed that  $t$  and  $n$  are held constant.

### 6.9.3.2 Combining the transfer equation

$$y_{+1} = y + tu,$$

with the above substitutions we have, for the case of  $t = \text{constant}$ ,

$$dy_{+1} = t du.$$

Using this and Equations (28) to (31), Equations (26) and (27) become

$$dy_k = \frac{n}{\Phi} (y_k \bar{y} - \bar{y}_k y) du, \quad (32)$$

and

$$du_{k-1} = \frac{n}{\Phi} (\bar{y} u_{k-1} - y \bar{u}_{k-1}) du. \quad (33)$$

6.9.3.3 Equation (13), defining the second focal length, assumes that the axial paraxial ray was traced at  $u_o = 0$ . Differentiating this equation, remembering that  $y_1$  is arbitrary and hence independent of  $c$ , we have

$$\frac{df'}{dc} = - \left( \frac{f'}{u_{k-1}} \right) \left( \frac{du_{k-1}}{dc} \right) = - \left( \frac{f'}{u_{k-1}} \right) \left( \frac{du_{k-1}}{du} \right) \frac{du}{dc}.$$

Differentiating 5-(57) it follows that

$$\frac{du}{dc} = \frac{y(n_{-1} - n)}{n}.$$

Therefore, using Equation (33),

$$\frac{df'}{dc} = \frac{[-f'(\bar{y} u_{k-1} - y \bar{u}_{k-1})][y(n_{-1} - n)]}{\Phi u_{k-1}}.$$



6.9.4 Effect of curvature change on final angle. In Table 6.12 a calculation is shown for a change in curvature made on the fourth surface of the example given in Table 6.6. Comparing the new  $u_6$  with the original one in Table 6.6 we have  $\Delta u_6 = 0.00469$ . Now we will compare this value with a calculated value using the equations for the differential coefficients. Since we are making a change in the curvature only, keeping the thickness and index constant, we calculate

$$\frac{du_{k-1}}{dc} = \frac{du_{k-1}}{du} \frac{du}{dc}$$

From Equation (32), and data from Table 6.6, the following calculation may be made,

$$\begin{aligned} \frac{du_6}{dc_4} &= \frac{y_4 (n_3 - n_4)}{\Phi} (\bar{y}_4 u_6 - y_4 \bar{u}_6) \\ &= - \frac{1.026 \times .621}{.5} (-0.00069 \times 0.08664 - 1.02606 \times 0.35886) \\ &= 0.469 . \end{aligned}$$

We have then that

$$\Delta u_6 = \frac{du_6}{dc_4} \Delta c_4 = (0.469) (0.01) = 0.00469 .$$

This is in exact agreement with the result from Table 6.12.

6.9.5 Effect of thickness change on final angle. It is also possible to compute the change in the final angle from a change in any thickness  $t$ . If  $t$  is changed, then,

$$dy_{+1} = u dt .$$

| SURFACE         | 4        | 5        | 6        | 7        |
|-----------------|----------|----------|----------|----------|
| c               | 0.26973  | 0.05065  | -0.24588 | 0        |
| t               | 1.13691  | 0.6      | 14.9709  |          |
| n               | 1.621    | 1        | 1.620    | 1        |
| $c(n_{-1} - n)$ | 0.16750  | -0.03140 | -0.15245 | 0        |
| $t/n$           | 1.13691  | 0.37037  | 14.9709  |          |
| y               | 1.02606  | 1.18794  | 1.22686  | 0        |
| nu              | -0.02948 | 0.14238  | 0.10508  | -0.08195 |

$$\Delta u_6 = -0.08195 - (-0.08664) = 0.00469$$

Table 6.12 - Calculations showing the effect on  $u_{k-1}$  of a change of  $\Delta c_4 = 0.01$  in the data in Table 6.6

Therefore, using Equation (27) with  $du = 0$ , and Equation (30),

$$\frac{du_{k-1}}{dt} = \frac{\partial u_{k-1}}{\partial y_{+1}} \frac{dy_{+1}}{dt},$$

and

$$\frac{du_{k-1}}{dt} = \frac{nu}{\Phi} \left[ \bar{u}_{k-1} u - u_{k-1} \bar{u} \right].$$

## 6.10 CHROMATIC ABERRATION

**6.10.1 The meaning of chromatic aberration.** The variation of refractive indices with wavelength was discussed under the topic of dispersion in Section 2.6. The method of differential coefficients described in Section 6.9 can be used to calculate the effect of such a change in the index of refraction of the lenses. This change in index affects the refraction of each ray so that rays of different wavelengths pass through the system in slightly different paths. Generally these rays of different wavelengths give rise to more than a single image, a phenomenon called chromatic aberration. If the images are at different positions along the optical axis, the system exhibits longitudinal or axial chromatic aberration. If the images are of different lateral magnification, the system exhibits transverse or lateral chromatic aberration. Axial and lateral chromatic aberrations are sometimes referred to as axial color and lateral color, respectively.

### 6.10.2 Surface contributions.

**6.10.2.1** As mentioned above, each surface introduces a certain amount of chromatic aberration appearing in the final image. The amount due to a particular surface is called the surface contribution. The general approach used to calculate first and third order aberrations is (1) determine the surface contribution, and (2) sum the contributions for all surfaces to find the total aberration. The individual contributions may be positive, negative, or zero. Hence the sum may be either positive, negative, or zero. In the last case the system would be free of this particular aberration.

**6.10.2.2** The first order chromatic aberration contribution of any surface may be found by differentiating Equation 5-(57), assuming that  $du_{-1} = 0$ . This assumption means that the ray between the  $j-1$  and  $j$ th surfaces is unaberrated; hence we are considering only the contribution of the  $j$ th surface. The assumption  $du_{-1} = 0$  also leads to  $dy = 0$ , because the ray to the left of the  $j$ th surface retains its original path. We then have,

$$n du + u dn = u_{-1} dn_{-1} + yc (dn_{-1} - dn).$$

This can be put into a form more suitable for calculation. From Equation 5-(35), written for small angles, and Equation 6-(4), we have

$$i' = yc + u. \tag{33a}$$

Using this equation, Equation 2-(1) for small angles, and Equation 6-(4), it is possible to derive the expression

$$du = i \frac{n_{-1}}{n} \left[ \left( \frac{dn_{-1}}{n_{-1}} \right) - \left( \frac{dn}{n} \right) \right].$$

**6.10.2.3** Here,  $dn$  and  $dn_{-1}$  represent infinitesimal changes in index due to an infinitesimal change in wavelength  $\lambda$ . The change in  $u$ , due to a change of  $dn_{-1}$  and  $dn$ , will thus cause the ray to take a deviated path to the image. The change  $dy_k$ , in the final image, may then be calculated from

Equation (32). Since  $y_k = 0$  for the axial ray, the value of  $dy_k$  is:

$$dy_k = - \frac{y \bar{y}_k n_{-1} i}{\Phi} \left[ \left( \frac{dn_{-1}}{n_{-1}} \right) - \left( \frac{dn}{n} \right) \right] ;$$

$$dy_k = - \frac{y n_{-1} i}{(n_{k-1} u_{k-1})} \left[ \left( \frac{dn_{-1}}{n_{-1}} \right) - \left( \frac{dn}{n} \right) \right] ;$$

$$dy_k = y n_{-1} i \left[ \Delta \frac{dn}{n} \right] / (n_{k-1} u_{k-1}) ; * \quad (34)$$

or

$$dy_k = - a / (n_{k-1} u_{k-1}) .$$

The above derivation could have been equally well carried out for the oblique paraxial ray giving

$$d\bar{y}_k = y n_{-1} \bar{i} \left[ \Delta \frac{dn}{n} \right] / (n_{k-1} u_{k-1}) = - b / (n_{k-1} u_{k-1}) \quad (35)$$

$$= dy_k \bar{i} / i . \quad (36)$$

**6.10.3 Total chromatic aberration.** Equation (34) gives the amount by which the image of an axial object point is displaced from the optical axis due to the  $j$ th surface. Similarly Equation (35) applies to the image of an object point off the axis. Both these equations give the transverse displacement in the final paraxial image plane due to changes  $dn_{-1}$  and  $dn$ . Now, if these changes are due to a change of wavelength  $d\lambda$ , changes  $dn$  and  $dn_{-1}$  occur at every surface in the lens. Each surface then contributes a  $dy_k$  and a  $d\bar{y}_k$ , and since they are all differentials, they are directly additive. The totals are

$$\text{total } dy_k = \text{TAch} = \frac{-1}{(n_{k-1} u_{k-1})} \sum_{j=1}^{j=k-1} a , \quad (37)$$

and

$$\text{total } d\bar{y}_k = \text{Tch} = \frac{-1}{(n_{k-1} u_{k-1})} \sum_{j=1}^{j=k-1} b , \quad (38)$$

where  $a$  and  $b$  are the chromatic surface coefficients. Note that Equation (34) has  $i$  while Equation (35) has  $\bar{i}$ . In all other terms the equations are identical. The symbols  $\text{TAch}$  and  $\text{Tch}$  have replaced  $dy_k$  and  $d\bar{y}_k$  as descriptive terms to indicate the total transverse chromatic effects. TAch is the abbreviation for transverse axial chromatic aberration. Tch is the abbreviation for transverse chromatic aberration. A sample calculation for  $\text{TAch}$  is included in Table 6.7.

#### 6.10.4 Particular wavelengths used to calculate chromatic aberration.

**6.10.4.1** The first order chromatic aberration, strictly speaking, is the infinitesimal change,  $dy_k$ , resulting from a change  $dn$  which is due to a change  $d\lambda$ . Therefore, in order to calculate the infinitesimals,  $\text{TAch}$  and  $\text{Tch}$ , it is necessary to know the index at all wavelengths. As was discussed in Section 2.6.3, indices are measured at only certain standard wavelengths. It is possible to interpolate between standard wavelengths, using an appropriate dispersion formula, in order to calculate the index, and hence the chromatic aberration, at any wavelength.

**6.10.4.2** However, in order to obtain accurate indices for ray tracing, it is customary to use only measured indices. Therefore in order to calculate  $dn$ , which is now considered a finite change, two wavelengths are chosen  $n_v$  and  $n_r$ . Then  $dn_{v-r} = n_v - n_r$ . [ $v$  and  $r$  indicate wavelengths at the ends (violet and red) of the visible region]. Then a wavelength  $\lambda_g$  between  $v$  and  $r$  is used as the reference index of refraction.  $\lambda_g$  is any wavelength in the middle part of the spectrum. The paraxial

\* $\Delta(dn/n)$  is defined as  $\left( \frac{dn}{n} \right) - \left( \frac{dn_{-1}}{n_{-1}} \right)$ . The use of  $\Delta$  is often used in optics to denote the difference between a quantity on the two sides of a refracting surface. For example,  $\Delta n = (n - n_{-1})$ .

rays are traced at wavelength  $\lambda_g$ . Therefore,

$$T\text{Ach}_{v-r} = (y_k)_v - (y_k)_r,$$

and

$$T\text{ch}_{v-r} = (\bar{y}_k)_v - (\bar{y}_k)_r.$$

The differences are measured in the paraxial image plane where  $(y_k)_g = 0$ . It should be pointed out that  $T\text{Ach}_{v-r}$  and  $T\text{ch}_{v-r}$  tell only the difference in  $y_k$  and  $\bar{y}_k$  for light at wavelengths  $\lambda_v$  and  $\lambda_r$ . In order to calculate other chromatic aberrations, for example  $(y_k)_v - (y_k)_g$ , the calculations are made with

$$dn_{v-g} = (n_v - n_g).$$

The wavelengths chosen for calculation, depend on the wavelength region of interest. Visual optical systems are usually calculated with

$$n_v = n_F,$$

$$n_g = n_D,$$

and

$$n_r = n_C.$$

6.10.5 Graphical interpretation of axial and lateral color.

6.10.5.1 In Figure 6.13 a simple lens is shown with an exaggerated amount of chromatic aberration. A simple converging lens, which is necessarily uncorrected for aberrations, is said to be undercorrected. When a particular aberration is made zero, or smaller than some predetermined tolerance, the lens system is said to be corrected. If the aberration of the system has a sign opposite to that of a simple converging

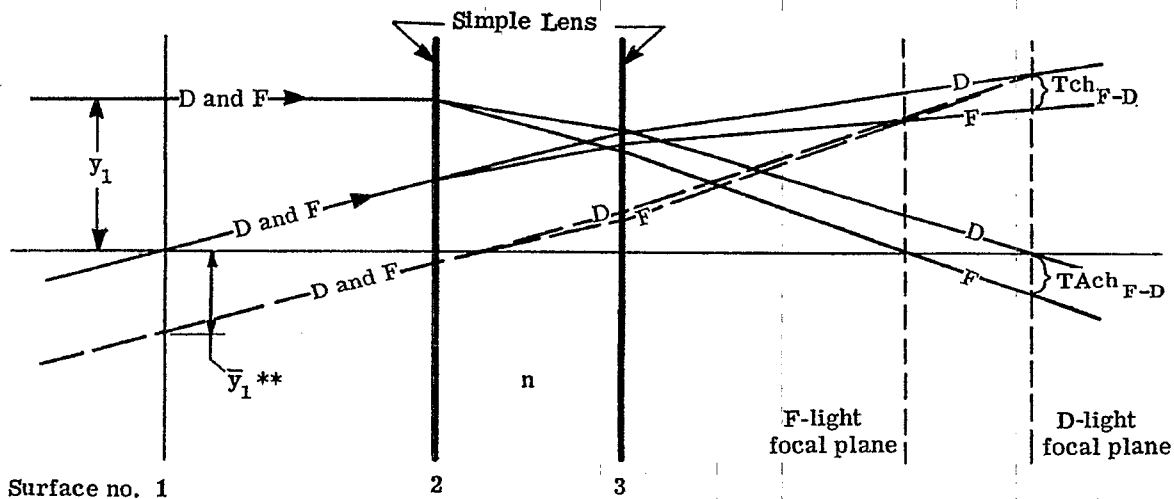


Figure 6.13 - Under-corrected chromatic aberration of axial and oblique rays in a simple lens.

lens, the system is over-corrected. The two surfaces of the lens in Figure 6.13 are labelled 2 and 3, and they appear as planes, as they should in the paraxial region. Axial and oblique rays in D and F light are shown as they pass through the lens. The oblique rays cross the axis at a reference surface #1. This reference plane will often coincide with the entrance pupil of the system. The pupils will be discussed in Section 6.11. With a positive lens, the F light image plane falls closer to the lens than the D light image plane. The chromatic blur,  $dy_{F-D}$ , is a linear function of  $y_1$ , the height of the axial ray entering the system. This can be seen by considering Figure 6.13. All axial paraxial rays in D light pass through the same point on the optical axis, independent of  $y_1$ . Hence all values of  $y_k$  for D light are zero and therefore Figure 6.14 indicates a horizontal line for D light. Similarly all axial paraxial rays in F light pass through a common point on the optical axis, independent of  $y_1$ . Hence the separation of the two focal planes for F light and D light is a constant, independent of  $y_1$ . This separation is called the longitudinal axial chromatic aberration, and is denoted by  $LA_{F-D}$ . From Figure 6.13 it is seen that

$$T\text{Ach}_{F-D} = (LA_{F-D}) u_{k-1} = - (LA_{F-D}) \frac{y_1}{f'}$$

Because the chromatic blur,  $T\text{Ach}_{F-D}$ , is a linear function of  $y_1$ , the line for F light in Figure 6.14 is straight and inclined to that for D light at the angle  $(LA_{F-D})/f'$ . Figure 6.14 shows a plot for  $(y_k)_F$  and  $(y_k)_D$  in the D light image plane, as a function of the height of the axial ray on the entrance pupil plane. This is a recommended way to indicate the transverse axial chromatic aberration of a system.

6.10.5.2 Figure 6.15 shows a plot of  $\bar{y}_k$  versus  $\bar{y}_1$  for F and D light. The chromatic blur,  $d\bar{y}_{F-D}$ , is a linear function of  $\bar{y}_1$  for a reason similar to that given in Paragraph 6.10.5.1. For all values of  $\bar{y}_1$ , all D rays pass through a common point on the D light focal plane. Similarly, all F rays pass through a common point. Since the rays are paraxial, the oblique ray at  $\bar{y}_1 = 0$  can be considered as an auxiliary axis; hence a ray parallel to it through a point  $\bar{y}_1 \neq 0$  will make the same angle with the chief ray that an axial paraxial ray makes with the optical axis. The former angle is a linear function of  $\bar{y}_1$ , as  $u_{k-1}$  is a linear function of  $y_1$ . Hence the chromatic blur is a linear function of  $\bar{y}_1$ , and the F light line is straight in Figure 6.15. The distance between the F and D chief rays in the D light image plane is as indicated in Figure 6.15. This is the value computed from Equation (38). The differ-

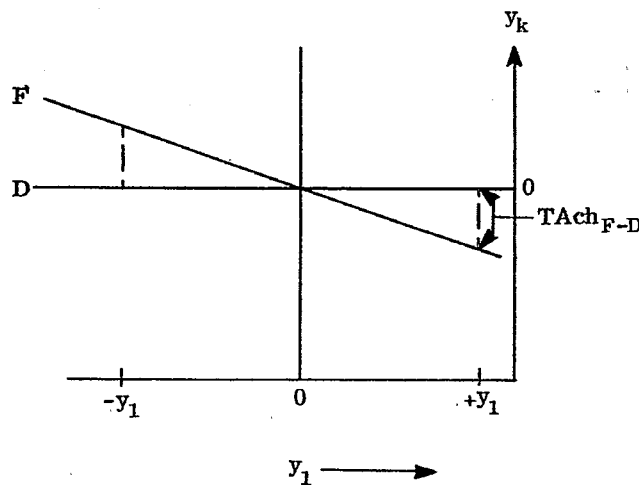


Figure 6.14 - A plot of  $y_k$  for F and D light versus the height  $y_1$  of the axial paraxial rays on the entrance pupil plane.

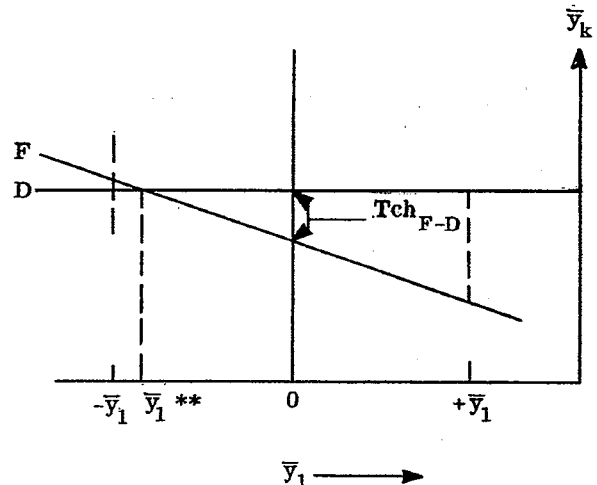


Figure 6.15 - A plot of  $\bar{y}_k$  for F and D light versus the height  $\bar{y}_1$  of the oblique paraxial rays.

ence in slope between the F and D lines is the same as for the axial rays shown in Figure 6.14, because the proportionality constant between T<sub>Ach</sub> and y<sub>1</sub> is identical to that between T<sub>ch</sub> and  $\bar{y}_1$ . Figure 6.15 (and also Figure 6.13) shows that there is a value of  $\bar{y}_1^{**}$  such that T<sub>ch F-D</sub> = 0. This means that if the oblique paraxial ray had been taken through the lens at a value of  $\bar{y}_1 = \bar{y}_1^{**}$ , instead of  $\bar{y}_1 = 0$ , then T<sub>ch F-D</sub> would come out to be zero. In fact, in general, it can be said that

$$Tch^*_{F-D} = Tch_{F-D} + \frac{\bar{y}_1^*}{y_1} T_{Ach}.$$

6.10.5.3 This equation states that T<sub>ch F-D</sub> can be calculated for any oblique ray striking the entrance pupil plane at  $\bar{y}_1^*$  with the above equation. The (\*) is used to indicate the T<sub>ch</sub> for some oblique ray displaced from the ray passing through  $\bar{y}_1 = 0$ . Defining  $\bar{y}_1^*/y_1 = Q$ , the above equation may be written

$$Tch^*_{F-D} = Tch_{F-D} + Q T_{Ach}. \tag{39}$$

Again it can be seen that it is necessary to trace only two paraxial rays through a lens system. It is possible to compute T<sub>Ach</sub>, and T<sub>ch</sub> for any other rays from the data on these two.

6.10.6 Basic concepts in correcting systems for chromatic aberrations.

6.10.6.1 If two wavelengths, F and D for example, come to focus in the same image plane, then  $(y_k)_F = (y_k)_D = 0$ . This equation gives the condition for correction of the axial color. However, this does not mean that  $(u_{k-1})_F$  will necessarily be equal to  $(u_{k-1})_D$ . If these two angles are not equal, then the magnifications between the object and image will not be equal, and  $(\bar{y}_k)_F \neq (\bar{y}_k)_D$ . Therefore, the system will have residual lateral color. Hence if both axial and lateral color are to be corrected, the rays in F and D light should emerge from the system at the same value of  $y_{k-1}$  and  $u_{k-1}$ .

6.10.6.2 The usual achromatic doublet lens is corrected for axial and lateral color because the axial rays in the F and D light never become significantly separated. See Figure 6.16 (a). In the case of two separated lenses, Figure 6.16 (b), it is clear that both elements must be color corrected, to keep the rays together all the way to the final image. If any axial color is allowed in the front element the rear element would have to be thick enough and designed properly to get the two rays together again before emerging from the rear surface. It is possible, by using the proper lens power and glass dispersion, to correct for axial and lateral color in widely spaced lenses as shown in Figure 6.16 (c). This is the principle used in the design of the famous Taylor triplet photographic lens. As a general principle, however, it is always advisable to keep the color rays as close together as possible at all times. This means, if the system is to be made up of several components, each component should be made achromatic.

6.10.7 Chromatic aberration in a thin lens.

6.10.7.1 It is possible to apply Equations (37) and (38) to a thin lens immersed in a non-dispersive medium and simplify the equations because the values of y and of  $\bar{y}$  are the same on both surfaces. Suppose there is a thin lens in a system of thin lenses in air with values of y and  $\bar{y}$  for heights of the axial and oblique paraxial rays. (See Figure 6.17). This lens will contribute the following amounts of axial and lateral color to the final image.

$$T_{Ach}_{v-r} = \frac{1}{(n_{k-1} u_{k-1})} \left( y^2 \frac{\phi}{\nu_{v-r}} \right),$$

and

$$Tch_{v-r} = \frac{1}{(n_{k-1} u_{k-1})} \left( y \bar{y} \frac{\phi}{\nu_{v-r}} \right).$$

where  $\phi$  is the power of the lens, and  $\nu_{v-r} = (n_g - 1)/(n_v - n_r)$ . These equations follow from Equations (37) and (38), with the use of Equations (4), (22), (33a) and 2-(1) for small angles.

6.10.7.2 Each of the thin lenses adds a contribution, so the final axial and lateral color for a system of  $\eta$

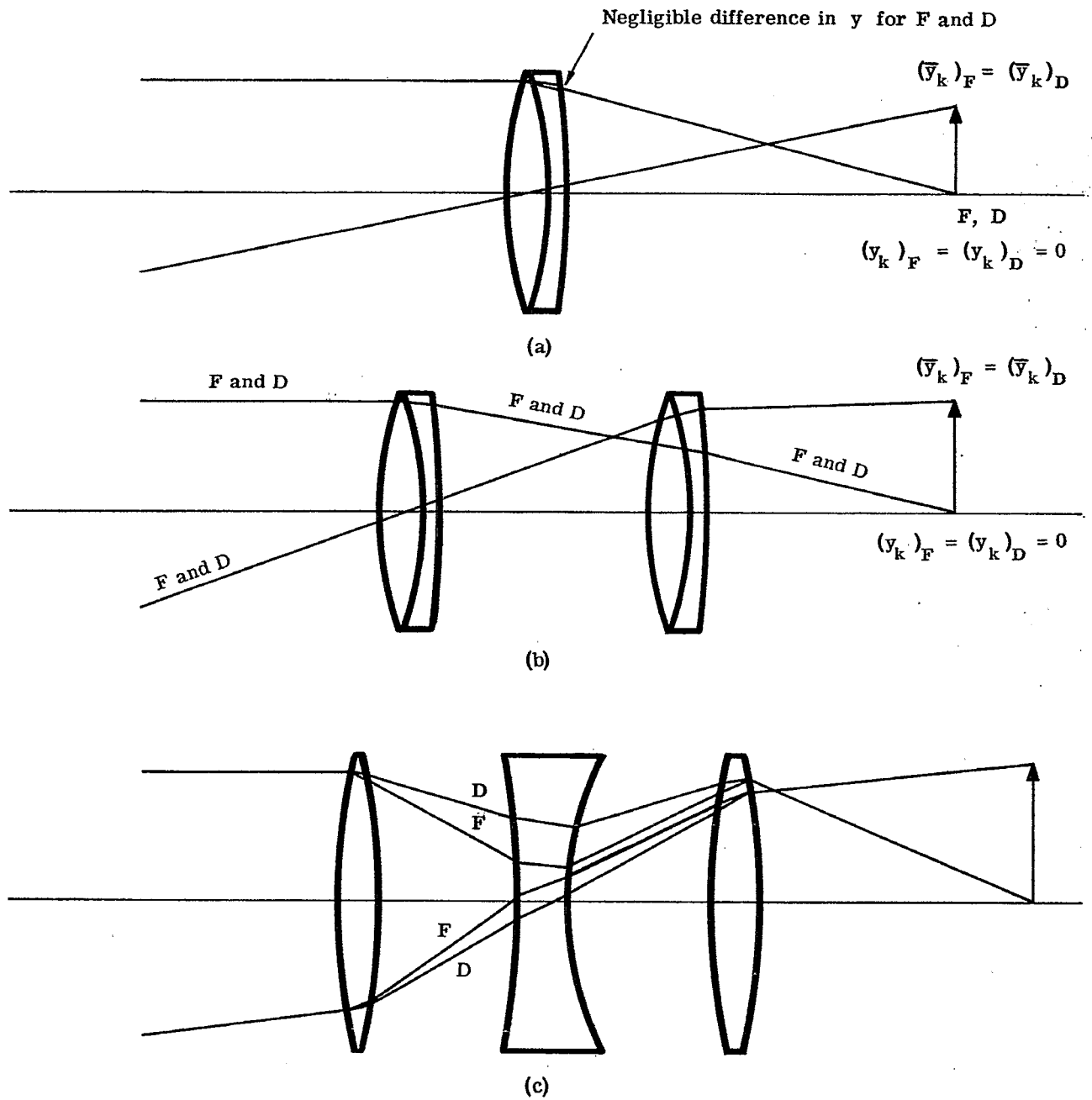


Figure 6.16 - Illustration of axial and lateral color correction for paraxial rays.

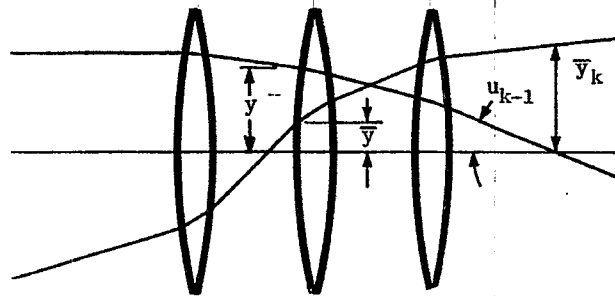


Figure 6.17 - A system of thin lenses.

| SURFACE                     | (1, 2)    | (3, 4)    | (5, 6)    | IMAGE                  |
|-----------------------------|-----------|-----------|-----------|------------------------|
| $-\phi$                     | -0.16537  | 0.28698   | -0.18208  |                        |
| t                           | 1.4685    | 1.4868    |           |                        |
| y                           | 1.5       | 1.1357    | 1.2515    |                        |
| u                           | 0         | -0.2481   | 0.0779    | -0.1500                |
| $\bar{y}$                   | -0.8      | -0.07119  | 0.63633   |                        |
| $\bar{u}$                   | 0.364     | 0.49630   | 0.47587   | 0.36000                |
| $\nu F-C$                   | 60.3      | 36.2      | 60.3      |                        |
| $a = -\frac{y^2 \phi}{\nu}$ | -0.006171 | 0.010226  | -0.004730 | $\Sigma a = -0.000675$ |
| $b = -\bar{y}y\phi/\nu$     | 0.003291  | -0.000641 | -0.002405 | $\Sigma b = 0.000245$  |

$$T_{Ach} = \frac{-\Sigma a}{(n_{k-1} u_{k-1})} = -0.00450$$

$$T_{ch} = \frac{-\Sigma b}{(n_{k-1} u_{k-1})} = 0.00164$$

Table 6.13 - Thin lens computation of axial and lateral color for a triplet. ( $f = 10$ )



thin lenses is given by,

$$T_{\text{Ach}}_{v-r} = \frac{1}{(n_{k-1} u_{k-1})} \sum_{j=1}^{\eta} \left( y^2 \frac{\phi}{\nu_{v-r}} \right)_j = \frac{-\sum a}{(n_{k-1} u_{k-1})}, \quad (40)$$

and

$$T_{\text{ch}}_{v-r} = \frac{1}{(n_{k-1} u_{k-1})} \sum_{j=1}^{\eta} \left( y \bar{y} \frac{\phi}{\nu_{v-r}} \right)_j = \frac{-\sum b}{(n_{k-1} u_{k-1})}. \quad (41)$$

The use of these equations is illustrated in Table 6.13. The system used in the table is very close to the thin lens equivalent of the system shown in Table 6.7. Note how the angle  $u$  of the axial ray as it passes through the system is the same, to four decimal places, for both examples. The  $T_{\text{Ach}}$  for the equivalent lens is not exactly the same as for the thick lens due to the thicknesses of the elements.

### 6.10.8 Thin lens achromatic system.

6.10.8.1 If Equation (40) is written for two closely spaced lenses (a) and (b), and combined, there results

$$T_{\text{Ach}}_{v-r} = \frac{1}{(n_{k-1} u_{k-1})} \left[ y^2 \left( \frac{\phi}{\nu_{v-r}} \right)_a + y^2 \left( \frac{\phi}{\nu_{v-r}} \right)_b \right]. \quad (42)$$

This is an expression for the axial chromatic aberration of the doublet lens. In order to make  $T_{\text{Ach}}_{v-r} = 0$ , it is necessary that,

$$\left( \frac{\phi}{\nu} \right)_a = - \left( \frac{\phi}{\nu} \right)_b. \quad (43)$$

In Table 6.9 it was shown that for two thin lenses in contact,

$$\phi = \phi_a + \phi_b.$$

Combining this equation with Equation (43) yields the relations,

$$\phi_a = \phi \frac{\nu_a}{\nu_a - \nu_b}, \quad (44)$$

and

$$\phi_b = -\phi \frac{\nu_b}{\nu_a - \nu_b}. \quad (45)$$

6.10.8.2 Equations (44) and (45) enable one to pick two glasses with different  $\nu$  - values and calculate the powers of the two lenses to make an achromatic lens. It is important to realize that these equations reduce the transverse axial chromatic aberration to zero only for the two wavelengths  $\lambda_v$  and  $\lambda_r$ . These are the two wavelengths used to compute the value of  $\nu$  for the glasses, where the  $\nu$  - number of a glass is defined as,

$$\nu_{(v-r)} = \frac{n_g - 1}{n_v - n_r}. \quad (46)$$

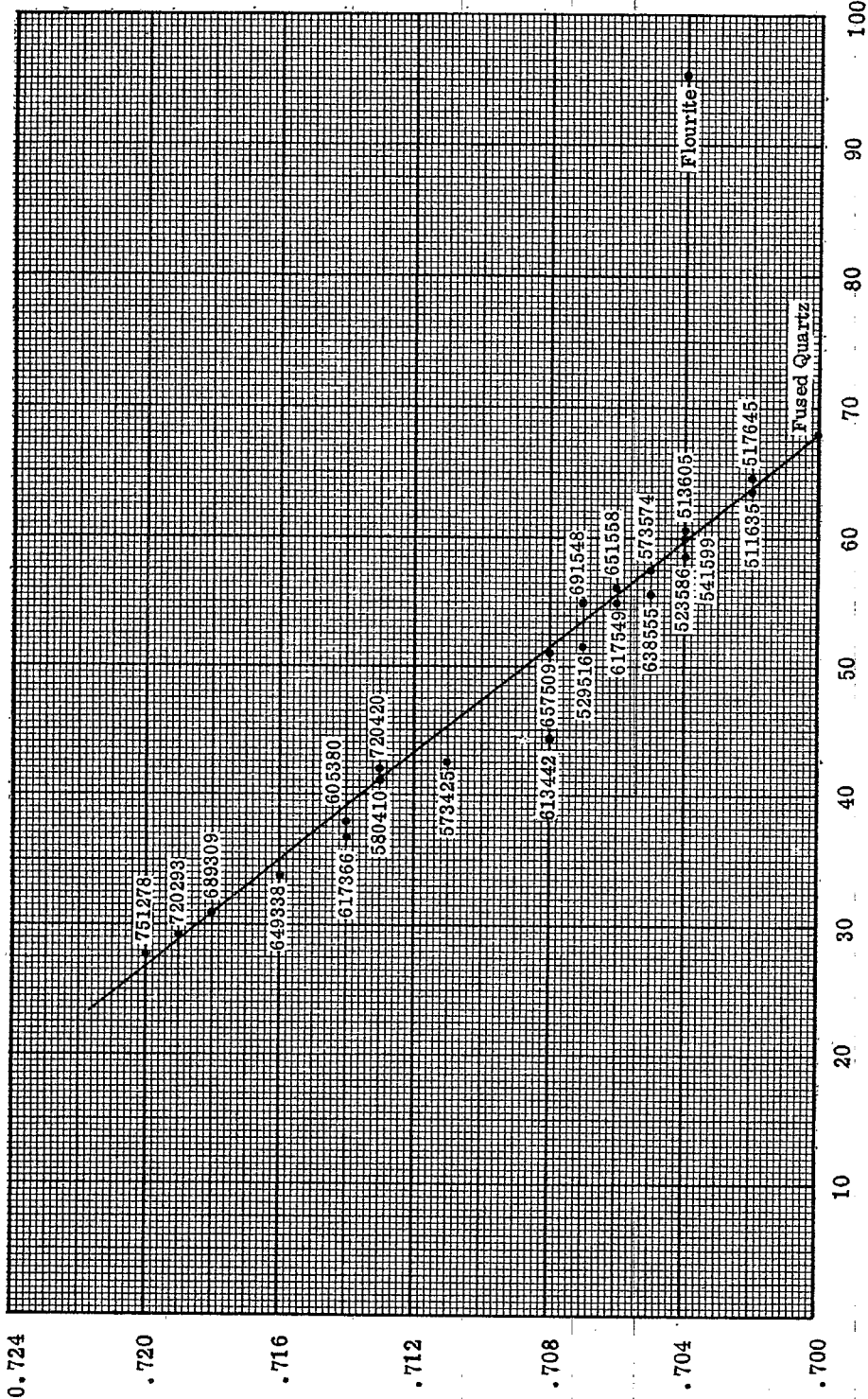
On the other hand, other wavelengths do not come to the same focus as  $\lambda_v$  and  $\lambda_r$ . The chromatic aberration  $T_{\text{Ach}}_{v-g}$  between an intermediate wavelength  $\lambda_g$  and  $\lambda_v$  may be calculated by substituting

$\nu_{v-g} = \frac{n_g - 1}{n_v - n_g}$  for each element and inserting them in Equation (42). Then

$$T_{\text{Ach}}_{v-g} = \frac{1}{(n_{k-1} u_{k-1})} \left[ y^2 \left( \frac{\phi}{\nu_{v-g}} \right)_a + y^2 \left( \frac{\phi}{\nu_{v-g}} \right)_b \right]. \quad (47)$$

Since the lens was adjusted to be an achromat for  $\lambda_v$  and  $\lambda_r$ , then Equation (43) must also be satisfied. This equation can be readily inserted in Equation (47) by an obvious redefining of  $\nu_{v-g}$ , as follows,

$$\nu_{v-g} = \left( \frac{n_g - 1}{n_v - n_g} \right) \left( \frac{n_v - n_r}{n_v - n_r} \right) = \nu_{v-r} \left( \frac{n_v - n_r}{n_v - n_g} \right).$$



$$\bar{P} = \frac{n_F - n_D}{n_F - n_C}$$

$$\nu = \frac{n_D - 1}{n_F - n_C}$$

Figure 6.18 -  $\bar{P}$  versus  $\nu_F - \nu_D$  for several glasses

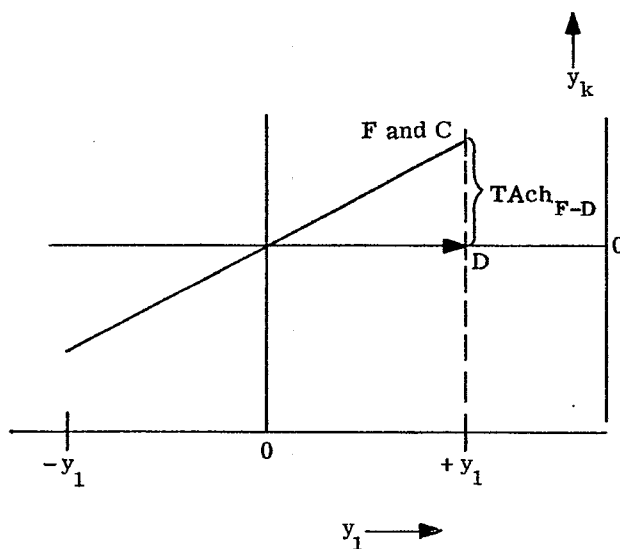


Figure 6.19 - Transverse axial chromatic aberration for an achromatic objective corrected for F and C light.

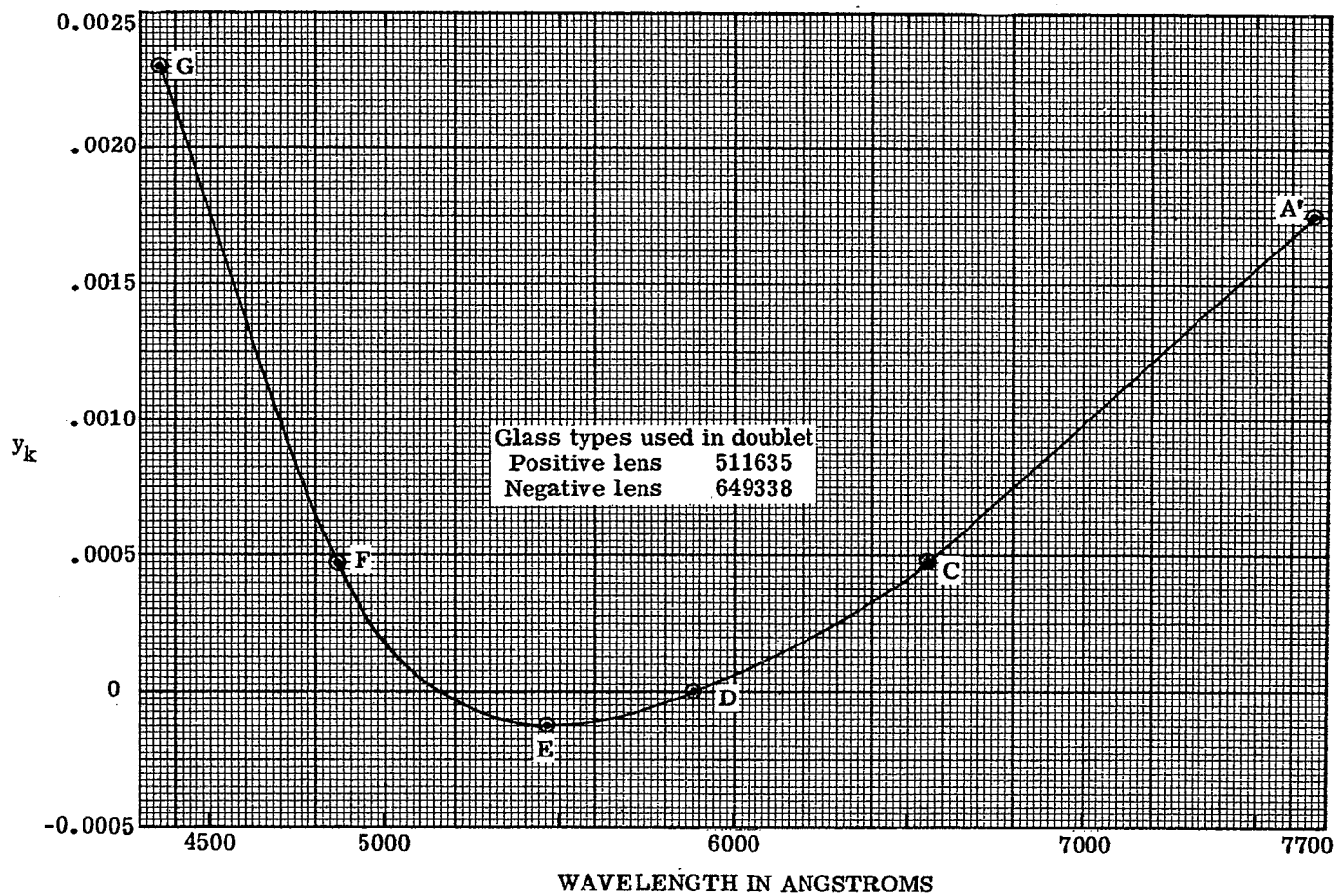


Figure 6.20 - Plot of  $y_k$  versus  $\lambda$  for an achromatic doublet.

Defining the partial dispersion ratio ( see Paragraph 2.7.3 ),

$$\tilde{P} = \frac{(n_v - n_g)}{(n_v - n_r)},$$

we have

$$\nu_{v-g} = \nu_{v-r} / \tilde{P}. \quad (48)$$

Equation (47) then becomes, with the help of Equations (44) and (45),

$$T\text{Ach}_{v-g} = \frac{-y}{n_{k-1}} \left[ \frac{\tilde{P}_a - \tilde{P}_b}{\nu_a - \nu_b} \right]. \quad (49)$$

6.10.8.3 Equation (49) gives the value of the transverse aberration between  $\lambda_v$  and  $\lambda_g$ , when  $\lambda_v$  and  $\lambda_r$  wavelengths are united. The equation indicates that if  $\lambda_v$ ,  $\lambda_g$ , and  $\lambda_r$  are to be brought to focus simultaneously, then  $\tilde{P}_a = \tilde{P}_b$ . Most glass catalogs give values of  $\tilde{P}$  for many combinations of wavelength for each glass. In Figure 6.18 the value of  $\tilde{P}$  for  $\frac{F-D}{F-C}$  is plotted against  $\nu_{F-C}$  for several types of glass. As will be pointed out in later sections, a doublet should be designed with low powers of the individual elements. Equations (44) and (45) show that the powers of the (a) and (b) elements of a doublet may be kept small by selecting optical glasses with large differences in  $\nu$ . Usually doublets should have  $\nu$  differences larger than 20. As can be seen from the slope of Figure 6.18, for almost any combination of glasses one can select, the ratio of  $(\tilde{P}_a - \tilde{P}_b) / (\nu_a - \nu_b)$  is a constant equal to  $-1/2200$ . When this number is substituted into Equation (49),  $T\text{Ach}_{v-g}$  is positive for positive  $y$ . Reference to Figure 6.13 indicates that for positive  $T\text{Ach}_{v-g}$  the axial ray in D light crosses the axis closer to the lens than the axial ray in F light. Using Equation (13) and noting that  $(u_{k-1})_F = (u_{k-1})_D$  to this approximation, we see that if F and C wavelengths are united, then D light focuses closer to the lens by the amount  $f'/2200$ , if the lens is in air. In Figure 6.19 a plot similar to that of Figure 6.14 is shown for a typical achromatic doublet, corrected to unite F and C light. It is instructive to plot the transverse axial aberration as a function of wavelength. This has been done in Figure 6.20 for an achromatic lens. Note how the curve has a minimum near  $\lambda = 5500\text{\AA}$ . This is the wavelength at the peak of sensitivity for the eye, which is the reason F - C achromatism is considered to be proper for visual systems.

6.10.8.4  $T\text{Ach}_{F-D}$  is called the secondary spectrum or the secondary color. It is a very difficult aberration to eliminate with ordinary glass types, and often sets the limiting aperture for a lens. The following methods may be used to reduce the secondary spectrum in a lens system.

- (1) Use special materials with equal partial dispersions.
- (2) Use more than two types of glass.
- (3) Use proper combinations of lenses.

More information on the correction of the secondary spectrum will be given in Section 11 under the design of telescope objectives. One can use Equation (40) to compute the secondary color for more complex optical systems, such as air spaced doublets, triplets, or combinations of doublets; however, the algebra becomes so complicated that it is difficult to obtain useful equations like (49) for anything more complicated than a closely packed doublet. It can be shown however, that for a given pair of glasses, the secondary color increases as the air space increases. The relation between secondary spectrum and separation of the two elements is derived by a method similar to that used for Equation (49). First an equation analogous to Equation (42) is derived; this will involve the separation of the elements as well as the powers and  $\nu$  - numbers. The condition for C - F achromatism, analogous to Equation (43) is then found. The total power for a dialyte from Table 6.9 is used with the achromatic condition to find the analogs of Equations (44) and (45). By the method given in 6.10.8.1, the equations analogous to (47) and (49) are then derived.

6.10.8.5 Although Section 6 deals with first order optics, and hence with the chromatic aberrations, we will mention here one of the third order aberrations, Petzval curvature, because of its close connection with the secondary spectrum. Petzval curvature, known also as curvature of field, has the following physical meaning. For monochromatic light, if spherical aberration, coma, and astigmatism are absent, the point images of point objects lie on a surface, generally curved. Near the optical axis this surface can be considered spherical with a curvature called the Petzval curvature. Flat-field systems have zero or very small Petzval curvature.

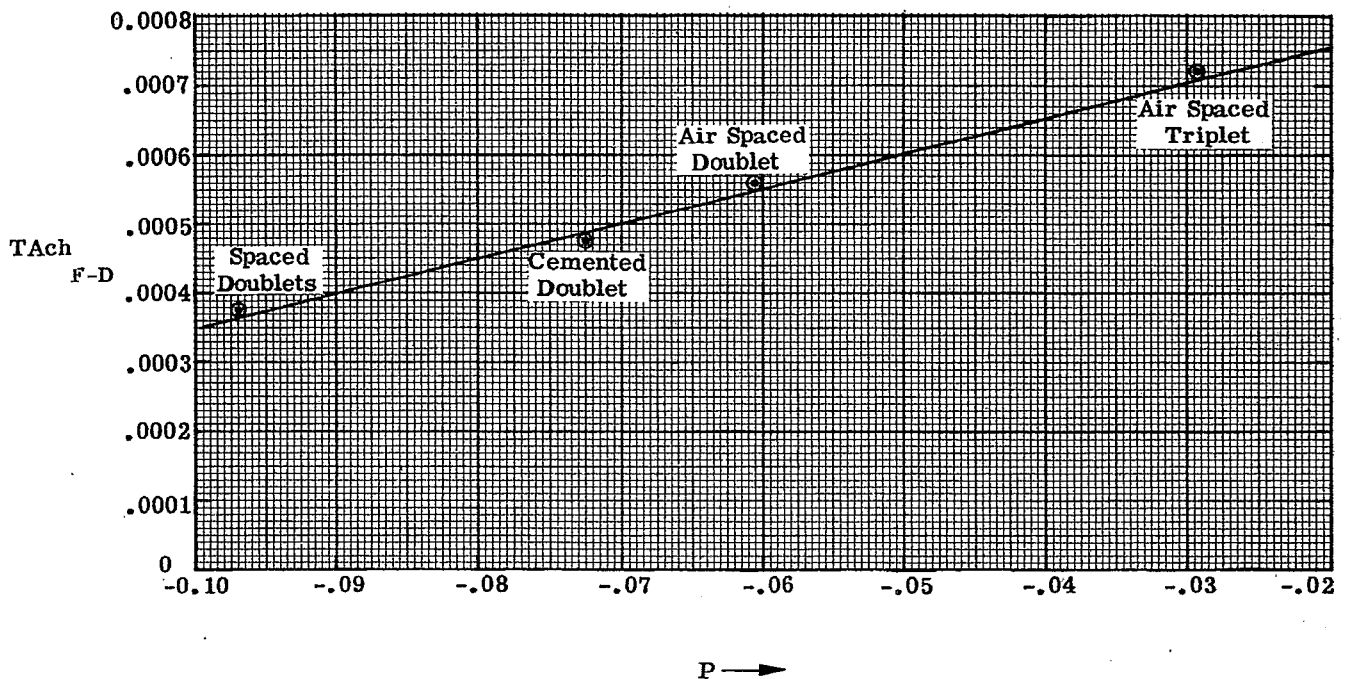


Figure 6.21 - Plot shows qualitative connection between Petzval curvature and secondary color. (Image is assumed in air).

6.10.8.6 Section 8 will discuss how the Petzval contribution for each surface is calculated. When the two surface contributions for a simple lens are added, as was done for the chromatic contributions in Paragraph 6.10.7.1, the Petzval contribution of a simple lens is  $P = -\phi/n$ . For a system of thin lenses in air,  $-P$  is the sum of the power,  $\phi$ , divided by the index for each lens.  $P = -\sum_{j=1}^n \frac{\eta_j}{n_j} \left( \frac{\phi_j}{n_j} \right)$ . If the

$TAch_{F-D}$  is plotted versus  $P$  for lens types, the points lie along an approximate straight line. This is shown in Figure 6.21. To obtain the data for this curve, a zero spaced doublet, an air spaced doublet, a positive-negative-positive-triplet, and two widely spaced achromatic doublets (a Petzval lens) were set up for computation. Each system has an exact focal length of 10 and is corrected for zero  $TAch_{F-C}$ . The axial paraxial ray was traced through at  $y = 1.0$ . All the positive lenses were of 511635 glass and all the negative lenses were of 649338 glass. This approximately linear relationship causes real difficulty in the design of flat-field lenses, since reduced Petzval curvature tends to accompany an increase in the amount of secondary color. This is a particularly serious problem in the design of periscope systems.

## 6.11 ENTRANCE AND EXIT PUPILS, THE CHIEF RAY AND VIGNETTING

6.11.1 **General.** As shown in Section 6.4, the complete analysis of the first order properties of an optical system can be found by tracing two rays through the optical system. Any two rays may be used, but it is convenient to pick the two rays with some care. In order to specify quantitatively which two rays are usually used, we must discuss the meanings of the pupils of an optical system.

6.11.2 **The aperture stop.** The bundle of rays, which proceed from an object point to the image point through an optical system, is limited in the sense that all the rays in the entire solid angle of  $4\pi$  steradians do not get through the system. The **aperture stop** is the physical stop or diaphragm, as distinguished from an image of a stop, which limits the rays passing through the system. The aperture stop may be a lens or it may be an opening in an otherwise opaque surface. It is almost always circular; we will consider it as such since we are concerned with systems having rotational symmetry.

### 6.11.3 Entrance and exit pupils.

6.11.3.1 The pupils are images of the aperture stop. The **entrance pupil** is the image of the aperture stop in the part of the system preceding the aperture stop. Hence to locate the entrance pupil, given the position of the aperture stop, an axial paraxial ray is traced backwards through the system from the center of the

aperture stop. The point where it last crosses the axis is the entrance pupil point. The entrance pupil plane is a plane perpendicular to the axis at the entrance pupil point. If the diameter of the aperture stop is known, an oblique paraxial ray is traced backwards from the rim or margin of the aperture stop. The intersection of this ray with the entrance pupil plane gives the radius of the entrance pupil.

6.11.3.2 Similarly, the exit pupil is the image of the aperture stop in that part of the system following the aperture stop. By tracing an axial and oblique ray from the aperture stop, the exit pupil plane can be located, and the diameter of the exit pupil can be determined. It sometimes happens that the aperture stop precedes (or follows) the rest of the system. In this case the aperture stop coincides with the entrance pupil (or exit pupil).

6.11.4 The chief ray. The chief ray is an oblique ray from an off-axis object point, which intersects the axis at the entrance pupil point, the center of the aperture stop, and the exit pupil point. Because it passes through the centers of the pupils and the aperture stop, it is approximately the central ray of the conical bundle from the object point to the image point. Hence it is representative of the entire bundle.

6.11.5 Two convenient paraxial rays. The usual procedure is to trace one ray from the point on the object plane intersected by the optical axis ( $y_0 = 0$ ). The angle with the optical axis,  $u_0$ , should be chosen to equal one half the actual cone angle to be passed by the optical system. Hence this ray passes through the margin of the pupils and the aperture stop.  $u_0$  is the radius of the entrance pupil divided by the distance between object surface and entrance pupil plane. The second ray should be traced from a point  $\bar{y}_0$  in the object plane corresponding to an object near the maximum size to be accommodated by the lens system. This second ray is a chief ray from the object point chosen. Hence  $\bar{u}_0$  is  $\bar{y}_0$  divided by the distance between object surface and entrance pupil plane. (See Figure 6.22).

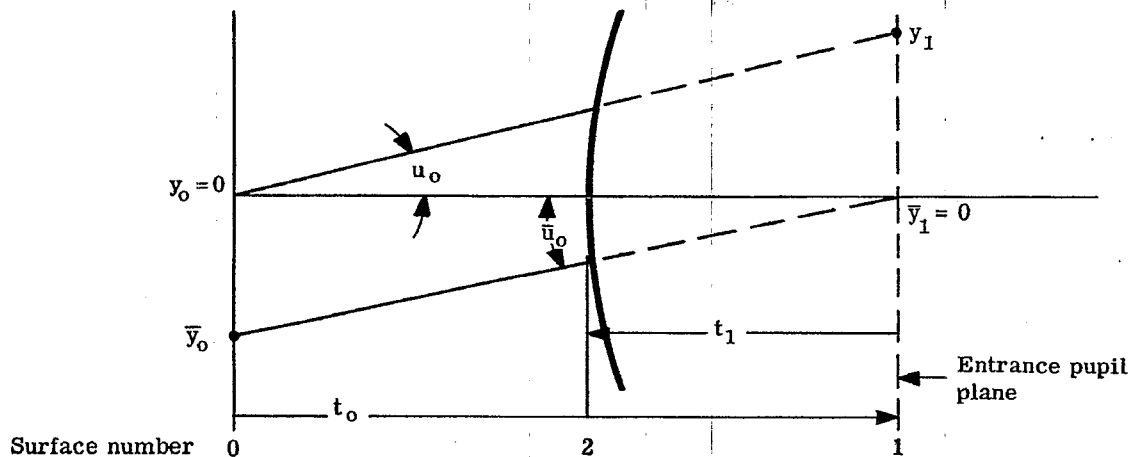


Figure 6.22 -Location of entrance pupil and numbering of surfaces.

6.11.6 Pupils as surfaces in the optical system. Many designers include the entrance pupil plane as a plane surface in the system. It is labelled number one. The actual first surface of the lens may be encountered before the chief ray reaches the entrance pupil. In this case the thickness  $t_1$  is made negative, indicating the entrance pupil plane is actually virtual. As the chief ray passes through the lens it may cross the axis at several positions. Each position is called an aperture plane. After it finally emerges in the image space it can be extended until it crosses the axis. This position is the exit pupil plane of the system and is numbered the  $(k - 1)$  surface. Although it is not necessary to include the entrance and exit pupil planes in the calculations of a lens, their inclusion is helpful because they are excellent planes of reference. It is convenient to describe aberration data by using the image coordinates plotted against their conjugate coordinates in the entrance pupil. (See Section 8).

6.11.7 Numerical example. As an example of the foregoing material, Figure 6.23 shows the pupils for a two-lens system. Table 6.14 shows the calculations for this system. In the example, the entrance pupil plane is found in the following way. As the chief ray is drawn, the lens (a) bends it up and the lens (b) bends it back down. It is nearly always true that  $(\Delta u_a + \Delta u_b)$  should be close to zero. This tends to keep the distortion corrected. (Distortion is a monochromatic aberration which will be discussed in Section 8). Since  $\Delta u = u - u_{-1}$ , Equation (24) shows that to meet this condition,  $y_a \phi_a + y_b \phi_b = 0$ .

The chief ray, therefore, must cross the axis between the two lenses and divide the space in the ratio of  $\phi_b / \phi_a$ . A value of  $-1$  for  $\bar{y}_a$  and  $+1$  for  $\bar{y}_b$  may be selected for convenience in this problem, because  $\phi_a$  and  $\phi_b$  are equal. Since  $t_2 = 5.0$ ,  $\bar{u}_2 = 0.4$ , and the chief ray can then be traced backwards to the object plane as shown in the example. The entrance and exit pupil planes are located by solving for  $t_1$  and  $t_3$  to make  $\bar{y}_1 = \bar{y}_4 = 0$ . Since  $\bar{y}_a = -1$  was used for convenience, the object height may come out to be far different from the value to be used for the true object. If the designer wishes to have a ray traced from the true object height, it may be done by simply scaling all the ray data for the chief ray. In the sample  $\bar{y}_o$  came out  $-4$ . A second ray was traced at  $\bar{y}_o = -2$ .

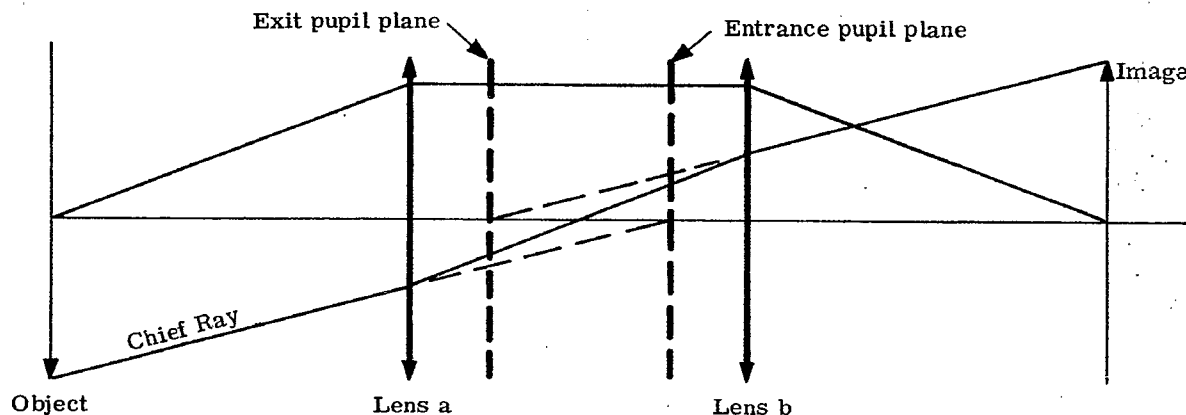


Figure 6.23 - Illustration of entrance and exit pupils.

| Surface   | Object Plane | Entrance Pupil Plane | Lens ( a ) | Lens ( b ) | Exit Pupil Plane | Image Plane |
|-----------|--------------|----------------------|------------|------------|------------------|-------------|
|           | 0            | 1                    | 2          | 3          | 4                | 5           |
| $-\phi$   | 0            | 0                    | -0.1       | -0.1       | 0                | 0           |
| $t$       | 13.33        | -3.33                | 5          | -3.33      | 13.33            |             |
| $y$       | 0            | 1.33                 | 1          | 1          | 1.33             | 0           |
| $u$       | 0.1          | 0.1                  | 0          | -0.1       | -0.1             |             |
| $\bar{y}$ | -4           | 0                    | -1         | 1          | 0                | 4           |
| $\bar{u}$ | 0.3          | 0.3                  | 0.4        | 0.3        | 0.3              |             |
| $\bar{y}$ | -2           | 0                    | -0.5       | 0.5        | 0                | 2           |
| $\bar{u}$ | 0.15         | 0.15                 | 0.2        | 0.15       | 0.15             |             |

Table 6.14 - Calculations showing location of entrance and exit pupil planes.

6.11.8 Vignetting.

6.11.8.1 In the above discussion on the aperture stop and pupils it was assumed that the aperture stop was circular. Hence the pupils are circular and a circular cone of rays passes through the system from an axial object point. For an off-axis object point, the cone of rays limited by the aperture stop will not be circular; and the entrance pupil will generally subtend at the object point a smaller solid angle than for an axial object point. This phenomenon is called vignetting; the oblique bundle of rays is said to be vignetted.

6.11.8.2 In the example shown in Table 6.14 the path of the chief ray has been calculated through a simple two-element lens. The next question is, what is the shape of the beam of light that passes through the optical system from the oblique object point? To answer this, it is necessary to project all the lens apertures in the system onto the entrance pupil plane. Since the path of any ray can be readily computed as a linear combination of two rays (see Section 6.4), it is possible to compute the coordinates in the entrance pupil plane for any ray from the object point of interest which passes through any part of any aperture of the system. For example, suppose we wish to find the coordinate on the entrance pupil plane of a ray from the object  $y_o = -2$ , which passes through the center of the (a) lens. Since two rays have been traced through the lens, a value of  $y$  and  $\bar{y}$  is known on each surface. Any other ray  $\bar{y}$  may be traced from the object point  $\bar{y}_o$  with the use of Equation (10a)

$$A \bar{y}_j + B y_j = \bar{y}_j .$$

On the object plane  $y_o = 0$ ,  $\bar{y}_o = \bar{y}_o$ . Therefore

$$A = \bar{y}_o / \bar{y}_o = 1 ,$$

and for the  $i$ th surface,

$$B = \frac{\bar{y}_i - \bar{y}_i}{y_i} .$$

Finally then,

$$\left[ \bar{y}_j - \bar{y}_j \right] = \left[ \bar{y}_i - \bar{y}_i \right] \frac{y_j}{y_i} . \quad (50)$$

To calculate the coordinate of any ray on the entrance pupil plane, which has the coordinate  $\bar{y}_i$  on the  $i$ th surface, Equation (50) becomes

$$\bar{y}_1 = (\bar{y}_i - \bar{y}_i) \frac{y_1}{y_i} ,$$

since  $\bar{y}_1 = 0$ .

6.11.8.3 In the example shown in Figure 6.23 and Table 6.14, a ray from the object point  $\bar{y}_o = -2$  passing through the center of the (a) lens ( $\bar{y}_2 = 0$ ) will project onto the entrance pupil plane at the value  $\bar{y}_1 = (0 + 0.5)(1.33)/1 = 0.666$ . The top edge of the (a) lens (assumed  $\bar{y}_2 = 1$ ) will appear in the entrance pupil plane at  $\bar{y}_1 = (1 + 0.5)(1.33) = 2$ . The center of the (b) lens will project in the entrance pupil plane at  $\bar{y}_1 = (0 - 0.5)(1.33) = -0.666$ . The top edge of the (b) lens (assume  $\bar{y}_3 = 1$ ) will appear in the entrance pupil plane at  $\bar{y}_1 = (1 - 0.5)(1.33) = 0.666$ .

6.11.8.4 Since the center and top edge of each lens, (a) and (b), are now projected on the entrance pupil plane, it is possible to construct circles indicating the complete aperture of the lenses as they appear in the entrance pupil plane. These apertures are shown in Figure 6.24. Only those rays passing through the area common to both circles will pass through the two lenses. In order to have the same aperture for the oblique beam as for the central beam, an aperture would have to be placed to appear as the inner circle shown in Figure 6.24. A circular aperture in the entrance pupil plane of radius 0.666 just fits in the common area of the two circles. Now in this case, the entrance pupil plane is virtual, so no physical stop can be placed in it. Since the chief ray does actually cross the axis at a point midway between the lenses, the physical aperture stop may be placed in this position and it will appear as a central stop in the entrance pupil plane. Using Equation (50), the size of the aperture stop can be calculated using the following data.

$$\bar{y}_1 = 0.666 = \text{height of edge of entrance pupil aperture.}$$

$$\bar{y}_i = \text{height of edge of aperture stop in the aperture plane.}$$

$$\bar{y}_i = 0 = \text{height of chief ray in the aperture stop plane.}$$

$$y_i = 1.0 = \text{height of axial ray in the aperture stop plane.}$$

$$y_1 = 1.33 = \text{height of axial ray in the entrance pupil plane.}$$

Therefore

$$\bar{y}_i = \frac{0.666}{1.33} = 0.5 .$$



6.11.8.5 Usually some vignetting for the oblique beams is allowed, so the aperture stop is made larger than the largest circle included in the common area. Figure 6.25 shows the appearance of the aperture stop when it is made 0.75 in radius. The clear area is the common area for all the apertures, and its area is a measure of the total light passing through the system from the oblique object point. The common area is 67% of the area of the image of the (0.75) aperture stop in the entrance pupil plane. Therefore, the oblique beam is vignetted by 33%. All other factors remaining constant, the illumination at the image point,  $\bar{y}_k = 2$ , is 67% of the illumination at the point  $y_k = 0$ . In Figure 6.25, the aperture stop of radius 0.75 located midway between the (a) and (b) lens, is imaged in the entrance pupil plane with a radius of 1.0. The exit pupil also has a radius of 1.0.

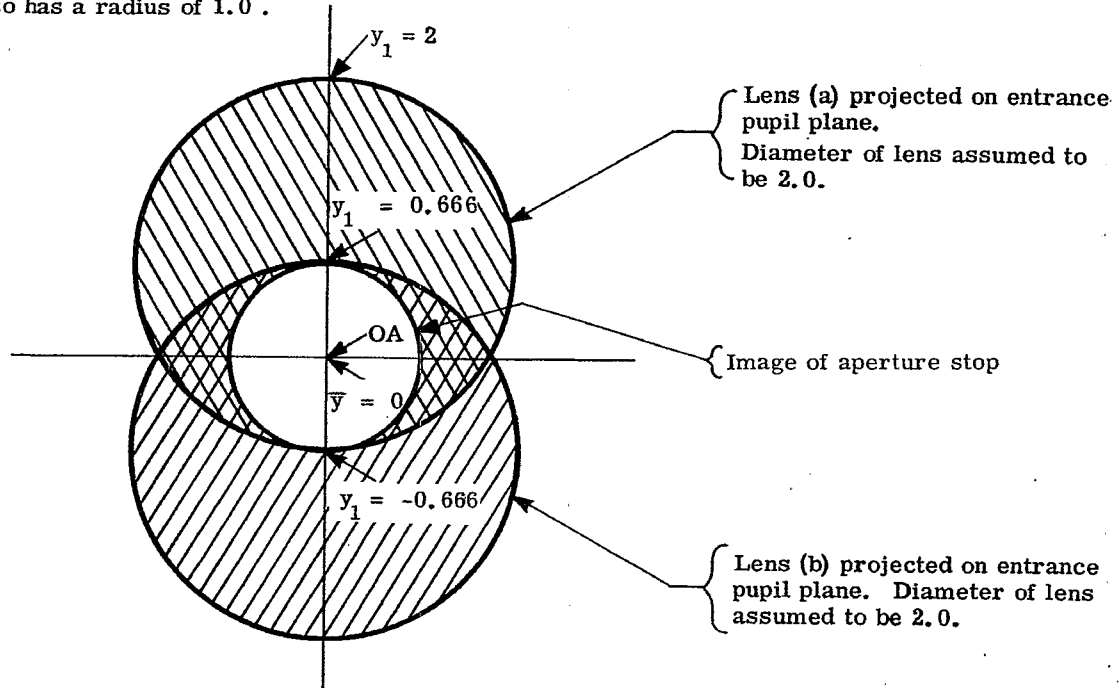


Figure 6.24 - Apertures of the (a) and (b) lenses and of the aperture stop projected onto the entrance pupil. The oblique beam is not vignetted.

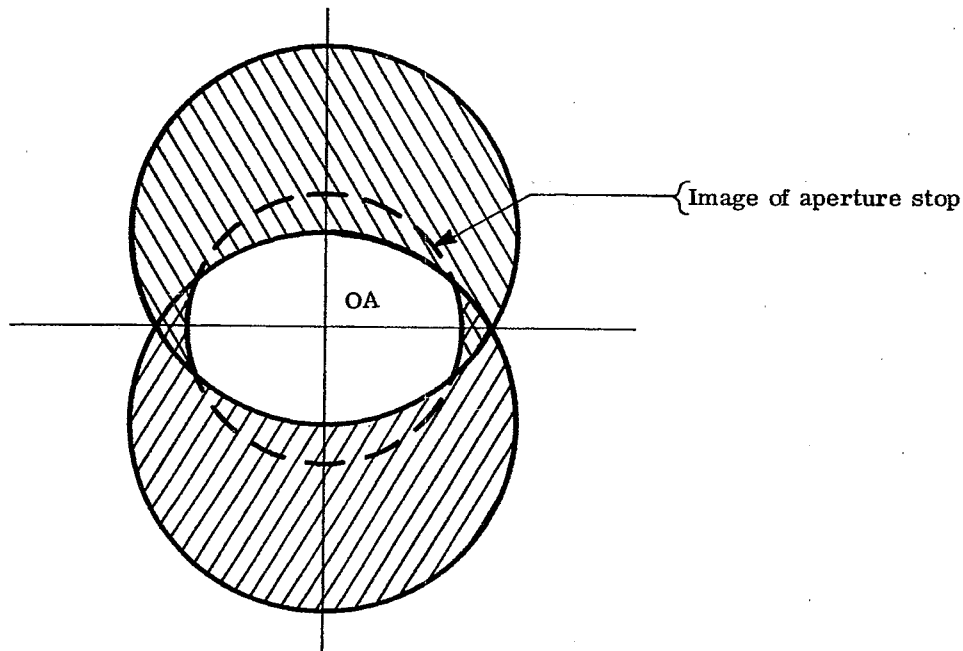


Figure 6.25 - Illustrating vignetting for the same system shown in Figure 6.24 but with a larger aperture stop.

